MASSACHUSETTS INSTITUTE OF TECHNOLOGY
RESEARCH LABORATORY OF ELECTRONICS
CAMBRIDGE, MASSACHUSETTS 02139

Final Report
covering the period
1 August 1981 — 31 May 1984

Sponsored by
Advanced Research Projects Agency
ARPA Order No. 4258

Program Code Number:
80230

Contract Number:
N00014-81-K-0662

Contractor:
Massachusetts Institute of Technology

Principal Investigator:
Jeffrey H. Shapiro

Scientific Officer:
Director Earth and Environmental Physics Program
Arctic and Earth Sciences Division
Office of Naval Research
800 North Quincy Street
Arlington, Virginia 22217

Title of Work:

Two-Photon Coherent State Light — Its Generation and Potential Applications

Effective Date of Contract:
August 1, 1981

Contract Expiration Date:
May 31, 1984

Amount of Contract:
$300,000

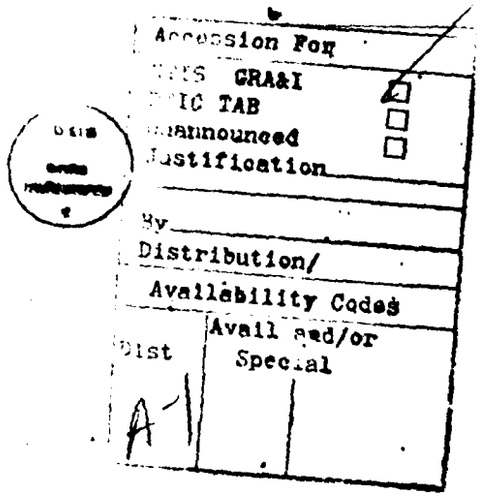

TWO-PHOTON COHERENT STATE LIGHT — ITS GENERATION AND POTENTIAL APPLICATIONS

Abstract

Recent work has highlighted the potential applications of two-photon coherent states (TCS), also known as squeezed states, in optical communications and precision measurements. This research program was aimed at generating TCS light via degenerate four-wave mixing (DFWM), and verifying the non-classical nature of TCS light via photon-counting measurements. The preceding experimental work was supported by analytical studies of DFWM TCS generation, and quantum photodetection. In addition, analyses were performed of key proposed TCS applications in optical communications and phase-sensing interferometry. Although the experimental effort did not yield any TCS observations, it did succeed in providing the first quantum-noise limited measurements obtained from DFWM. Moreover, the associated theoretical effort clarified pump quantum noise, probe-conjugate loss, and backward vs forward DFWM issues in TCS generation. Furthermore, the applications research developed simultaneous amplitude and phase uncertainty relations for optical heterodyne detection, and showed explicitly how to use TCS to surpass the so-called standard quantum limit (SQL) on position sensing in a gravity-wave detecting interferometer.

RESEARCH SUMMARY

A highly stabilized laser produces a light beam in a Glauber coherent state. This means the beam is endowed with the following quantum fluctuation behavior: photon counting measurements are Poisson distributed hence the count variance equals the count mean; and homodyne measurements are Gaussian distributed with signal-to-noise ratio equal to four times the average number of received photons. Furthermore, the observed fluctuation behavior for any laser, light-emitting diode, or ordinary light source can be accounted for by averaging the preceding results over a classical ensemble representing the light beam as a random mixture of coherent states. These results form the foundation for all of the semiclassical optical detection and communication analyses.

Recent theory has shown that the generation of light beams with quantum states of superior fluctuation behavior, relative to Glauber coherent states, may be possible. These states are called two-photon coherent states (TCS), or squeezed states. They are basically minimum uncertainty states for the quadrature components of the electromagnetic field possessing an asymmetric noise division between the quadratures, so that one quadrature has a "squeezed" noise variance, i.e., it is less than the coherent state value of 1/4. In photon counting measurements at high mean counts TCS light can have a count variance as low as $N_s^{2/3}$, where N_s is the average number of received photons. In homodyne measurements, because of the quadrature noise squeezing, TCS light can have a signal-to-noise ratio as high as $4N_s(N_s+1)$.

Under this research program, we have undertaken an experimental effort aimed at generating TCS light, and verifying some of its novel fluctuation characteristics [1] - [5]. In concert with the experimental activity, we have worked toward improving the theory behind TCS generation schemes [5] - [7],

advancing understanding of quantum photodetection (especially as applied to TCS light) [8], [9], and analyzing potential applications of TCS in optical communications [10] and phase-sensing interferometry [11], [12].

TCS Generation — Theory

Two-photon coherent states may be generated, in principle, by a variety of nonlinear optical processes, including the degenerate parametric amplfier (DPA) and degenerate four-wave mixing (DFWM). The essence of generating TCS may be stated simply as follows. For a single-mode field with annihilation operator $\hat{a}$, mix a part of this field with its phase conjugate field represented by the creation operator $\hat{a}^\dagger$ to create a new mode represented by the operator $\hat{c}$ such that

$$\hat{c} = \mu\hat{a} + \nu\hat{a}^\dagger , \qquad \text{(II.1)}$$

where $|\mu|^2 - |\nu|^2 = 1$ ensures that $\hat{c}$ is an annihilation operator. Then, if the mode $\hat{a}$ is in a coherent state (CS), the mode $\hat{c}$ will be in a TCS. Thus, a physical process that generates a phase conjugate field for some input field is a possible candidate for generating TCS light. DFWM is such a process, and was suggested by Yuen and Shapiro [13] as a possible source of TCS. In the standard backward DFWM geometry treated in [13], two counter-propagating pump waves intersect an object (probe) wave at a small angle in a nonlinear medium possessing a third order ($\chi^{(3)}$) nonlinearity. All three waves are at the same frequency. A phase-matched interaction in the nonlinear medium generates a phase-conjugate (PC) image wave which propagates in the opposite direction to the object wave. The outputs of the four-wave mixer can then be separated by means of isolators, and combined through an optical delay line with the proper phase relationships on a 50/50 beam splitter. In a classical analysis, the complex field amplitudes, A_1 and A_2,

of the image and object waves obey the coupled-mode equations

$$\frac{dA_1}{dz} = i\kappa^* A_2^* , \tag{II.2a}$$

$$\frac{dA_2}{dz} = -i\kappa^* A_1^* , \tag{II.2b}$$

where $\kappa^* = 2^{-1}\omega\chi^{(3)}B_1B_2/cn$ gives the complex coupling constant in terms of the nondepleted pump waves of complex field amplitudes B_1 and B_2. Yuen and Shapiro [13] gave a quantum version of the above treatment assuming that the pump fields B_1 and B_2 are strong and can remain classical along with the medium described by the third-order nonlinear susceptibility $\chi^{(3)}$. They quantized the object and the image modes replacing A_j and A_j^* with the photon annihilation and creation operators $\hat{a}_j$ and $\hat{a}_j^\dagger$, respectively, for $j = 1, 2$. Equation (II.2) then becomes

$$\frac{d\hat{a}_1}{dz} = i\kappa^* \hat{a}_2^\dagger , \tag{II.3a}$$

$$\frac{d\hat{a}_2}{dz} = -i\kappa^* \hat{a}_1^\dagger , \tag{II.3b}$$

with the following solutions

$$\hat{a}_1(0) = \mu\hat{a}_1(L) - i\nu\hat{a}_2^\dagger(0) , \tag{II.4a}$$

$$\hat{a}_2(L) = \mu\hat{a}_2(0) - i\nu\hat{a}_1^\dagger(L) , \tag{II.4b}$$

where $\mu = \sec(|\kappa|L)$, $\nu = e^{-i\theta}\tan(|\kappa|L)$, $\kappa = |\kappa|e^{i\theta}$, $\hat{a}_1(L)$ and $\hat{a}_2(0)$ are the input fields to the four-wave mixer at $z = L$ and $z = 0$, respectively.

When the outputs of the four-wave mixer are combined through a 50/50 beam splitter to generate two new modes

$$\hat{c} = [\hat{a}_1(0) - i\hat{a}_2(L)]/2^{1/2} , \tag{II.5a}$$

$$\hat{d} = [\hat{a}_1(0) + i\hat{a}_2(L)]/2^{1/2} , \tag{II.5b}$$

the solutions become

$$\hat{c} = \mu\hat{c}_{in} - \nu\hat{c}_{in}^{\dagger} \tag{II.6a}$$

$$\hat{d} = \mu\hat{d}_{in} - \nu\hat{d}_{in}^{\dagger} \tag{II.6b}$$

in terms of

$$\hat{c}_{in} = [\hat{a}_1(L) - i\hat{a}_2(0)]/2^{1/2} , \tag{II.7a}$$

$$\hat{d}_{in} = [\hat{a}_1(L) + i\hat{a}_2(0)]/2^{1/2} , \tag{II.7b}$$

which are linear combinations of the input modes to the four-wave mixer. Equation (II.6) is of the same form as (II.1) and $|\mu|^2 - |\nu|^2 = 1$, so that the modes $\hat{c}$ and $\hat{d}$ are in TCS if $\hat{a}_1(L)$ and $\hat{a}_2(0)$ are in CS.

The above analysis indicates that backward DFWM is a source of pure TCS. Depending upon the phase and magnitude of ν, arbitrary noise squeezing is predicted to be obtained in one of the quadratures of mode $\hat{c}$ or mode $\hat{d}$. In a real experiment, this is not quite so because of the assumptions made in arriving at (II.3). In particular, the pump modes B_1 and B_2 cannot necessarily be considered classical, and the effects of their quantum amplitude and phase fluctuations on modes $\hat{c}$ and $\hat{d}$ should be calculated. Moreover, the preceding analysis neglects loss, which is known to have a strong effect on quantum statistics.

In [5], [6] we have reported our analyses of generalizing the Yuen and Shapiro model to encompass pump quantum noise in a lossless backward DFWM setup, and loss on the probe and conjugate beams in backward DFWM in the absence of pump quantum noise. Both of these studies focused on the quadrature noise squeezing in the output modes $\hat{c}$ and $\hat{d}$ from (II.6). In particular, for the quadrature variance $\langle \Delta\hat{c}_1^2 \rangle \equiv \langle \Delta[(\hat{c}+\hat{c}^{\dagger})/2]^2 \rangle$ it was shown that the Yuen and Shapiro result is obtained in a lossless case with pump quantum

noise included if the pump beams are very intense ($|B_1| = |B_2| \rightarrow \infty$) the coupling is very weak ($2^{-1}\omega\chi^{(3)}/cn \rightarrow 0$) and the gain is constant ($|\kappa|L$ = constant). Thus, pump quantum noise places no fundamental limitation on TCS generation.

The results obtained for $\langle \Delta\hat{c}_1^2 \rangle$ in backward DFWM with probe-conjugate loss were not so favorable. Here it was found that even a moderate amount of such loss (e.g., loss coefficient $\gamma = 0.5/L$) severely limited the obtainable noise squeezing. Thus, loss presents a severe restriction on the use of resonant-medium backward DFWM as a TCS generator.

In an attempt to circumvent the preceding limitation, we turned our attention from backward DFWM to forward DFWM [7]. In forward DFWM, two strong pump beams propagate at small angles $\pm \phi/2$ from the +z axis in a $\chi^{(3)}$ medium. A phase matched interaction ensues between probe and conjugate waves at angles $\pm \phi/2$ from the +z axis in a plane obtained by rotating the pump-beam plane through an arbitrary angle about the z axis. This nominally co-propagating geometry, when analyzed quantum mechanically along the lines of the Yuen and Shapiro backward DFWM case, yields

$$\hat{a}_1(L) = \mu\hat{a}_1(0) - i\nu\hat{a}_2^{\dagger}(0) \ , \tag{II.8a}$$

$$\hat{a}_2^{\dagger}(L) = \mu\hat{a}_2^{\dagger}(0) + i\nu^{*}\hat{a}_1(0) \ , \tag{II.8b}$$

for the output annihilation operators at $z = L$ in terms of the input annihilation operators at $z = 0$, where $\mu = \cosh(|\kappa|L)$, $\nu = e^{-i\theta}\sinh(|\kappa|L)$, and $\kappa = |\kappa|e^{i\theta}$. Defining new output and input modes via (cf. (II.6), (II.7))

$$\hat{c} = [\hat{a}_1(L) - i\hat{a}_2(L)]/2^{1/2} \ , \tag{II.9a}$$

$$\hat{d} = [\hat{a}_1(L) + i\hat{a}_2(L)]/2^{1/2} \ , \tag{II.9b}$$

and

$$\hat{c}_{in} = [\hat{a}_1(0) - i\hat{a}_2(0)]/2^{1/2} , \qquad \text{(II.10a)}$$

$$\hat{d}_{in} = [\hat{a}_1(0) + i\hat{a}_2(0)]/2^{1/2} , \qquad \text{(II.10b)}$$

yields

$$\hat{c} = \mu\hat{c}_{in} - \nu\hat{c}_{in}^{\dagger} , \qquad \text{(II.11a)}$$

and

$$\hat{d} = \mu\hat{d}_{in} + \nu\hat{d}_{in}^{\dagger} . \qquad \text{(II.11b)}$$

Thus, for lossless forward DFWM with no pump quantum noise ideal TCS generation results from 50/50 interferometric combination of the two output beams.

We have not explicitly examined the pump quantum noise behavior of forward DFWM; we expect it will mimic that of backward DFWM. We have shown, however, that probe-conjugate loss does not present a fundamental limit on obtainable quadrature noise squeezing from forward DFWM. This is because the counter-propagating geometry of backward DFWM causes a looping of loss-induced quantum noise in the interaction medium that is absent in the co-propagating geometry of forward DFWM. Thus, forward DFWM is a more promising TCS generator than is backward DFWM.

TCS Generation - Experiment

We chose to pursue TCS generation experimentally via backward DFWM in sodium vapor. (This work was initiated before our loss analysis was completed.) Because DFWM occurs through the third-order nonlinearity $\chi^{(3)}$ of the mixing medium, we employed a pulsed optical system and exploited the resonant enhancement of sodium $\chi^{(3)}$ in the vicinity of 589 nm wavelength D_2 transition in order to access the high reflectivity regime. Furthermore, because a pulsed experiment did not lend itself to homodyne detection, we

used photon counting to look for anti-bunching (i.e., second reduced factorial moment g_2 less than unity) in light that had undergone DFWM. No previous DFWM experiments had ever tried to look at quantum noise; it turned out that our initial DFWM quantum-noise experiment was overconstrained by a combination of factors, as elaborated below.

The experiment comprised three subsystems: a continuous-wave oscillator/pulsed-amplifier chain dye laser, a heat-pipe oven sodium vapor cell, and a special purpose photomultiplier tube/computer data acquisition photon counting setup. The laser system [2] was developed to approach insofar as possible the stable center-frequency transform-limited pulse train needed for eliminating classical excess fluctuations in the DFWM conjugate output beams [4]. The photon counting system [1] was assembled to permit accurate photon statistics determination from the nanosecond duration pulses produced by the laser. As described in [3], [5] background light from the sodium cell had to be reduced to less than one detected photon per pulse, by means of spatial filtering, time gating, and adjustment of DFWM pump strength and pump/probe angular separation, in order to make the desired quantum noise measurements. The result was that we had to operate in a low-reflectivity regime for which Poisson statistics (g_2=1) were expected. Our measurements confirmed the Poisson behavior [3], [5], indicating that we were able to reduce excess fluctuations to acceptably low levels, thus demonstrating the first quantum-limited noise measurements obtained on a DFWM output beam.

Quantum Photodetection

As an adjunct to the detection aspects of the TCS generation work, and as a foundation for TCS applications research in optical communications and precision measurements, a number of new theoretical results were developed in the area of quantum photodetection. Building from Cook's photon flux picture of photodetection [14], we relaxed [8], [9] the quasimonochromatic

condition in Yuen and Shapiro's operator representations [15] for direct detection, homodyne detection, and heterodyne detection, and extended [8] the coherent detection results of [15] to include dual detection configurations (cf. [16]) and local oscillator excess noise. Moreover, the results of [8] were couched in terms which made comparison with familiar multi-mode semi-classical shot noise particularly simple. Finally, in [9], we showed that multi-mode TCS permit heterodyne detection amplitude and phase measurements to be made simultaneously without being subject to any uncertainty principle. This phenomenon has applications in precision measurements (see below).

Optical Communications with TCS

Helstrom [17], [18] found the optimum quantum measurement operator for deciding between equally likely density operators ρ_0 and ρ_1 for the state of a quantized signal field to be as follows. The minimum error probability decision rule chooses hypothesis H_j (i.e., state ρ_j) when the outcome of measuring $u(\rho_1 - \rho_0)$ is j, where $u(\times)$ is the unit step function. Helstrom also showed that the error probability of this receiver obeys

$$Pr(e) = 2^{-1}\{1 - [1 - |\langle \Psi_1|\Psi_0\rangle|^2]^{1/2}\} , \qquad (II.12)$$

for the pure state problem $\rho_j = |\Psi_j\rangle\langle\Psi_j|$. Kennedy [19] and Dolinar [20] later deduced realizations for exponentially optimum and exactly optimum receivers, respectively, when the $|\Psi_j\rangle$ are coherent states, using conditional Poisson process photodetection models. Shapiro [21], using the representation theorem from [15], was able to explicitly develop the operator description of the near-optimum receiver. In this program we have extended the work of Kennedy, Dolinar, and Shapiro to the detection of binary two-photon coherent state signals.

In comparison with coherent state signals TCS offer significant communication performance advantages, e.g., (II.12) reduces to

$$\Pr(e) = \begin{cases} 2^{-1}\{1 - [1 - \exp(-4N_s)]^{1/2}\}\ , \\ \qquad\qquad \text{for coherent state } |\Psi_j\rangle \\ \\ 2^{-1}\{1 - [1 - \exp(-4N_s(N_s+1))]^{1/2}\}\ , \\ \qquad\qquad \text{for optimized TCS } |\Psi_j\rangle\ , \end{cases} \tag{II.13}$$

of average energy content N_s photons. We have developed a general explicit realization for the $u(\rho_1 - \rho_0)$ measurement for TCS signals [10]. Our construction of the optimum TCS measurement combines the operator transformation properties of the idealized four-wave mixer in [13] first with the near-optimum operator analysis in [21] and later with a quantum version of the Dolinar work [20].

Phase-Sensing Interferometry

The performance of phase-sensing interferometers employing TCS and homodyne detection were analyzed [11], [12] and compared to the performance of systems employing direct detection [22]. Standard differenced direct-detection Michelson and Mach-Zehnder interferometers were shown to be sub-optimal in the sense that an observation/measurement-noise coupling occurs, which can degrade performance. Homodyne-detection interferometers in which the phase shift in one arm is the conjugate of that in the other arm do not suffer from the preceding drawback. Overall, however, the performance of differenced direct-detection and homodyne-detection interferometers is similar in single-frequency operation. In particular, both detection schemes reach the standard quantum limit on position measurement sensitivity in single-frequency interferometric gravity-wave detectors at roughly the same average photon number. This limit

arises from back action in the form of radiation pressure fluctuations entering through the energy-phase uncertainty principle. Multi-frequency devices can circumvent this uncertainty principle, as was illustrated by the conceptual design we have given for a two-frequency interferometer which can greatly surpass the standard quantum limit on position sensing. This interferometer relies on the heterodyne results developed in [9], and complements recent work of Yuen [23] on the validity of the position-sensing SQL.

REFERENCES

[1] R.S. Bondurant, P. Kumar, J.H. Shapiro, and M.M. Salour, "Photon Counting Statistics of Pulsed Light Sources," Opt. Lett. 7, 529-531 (November 1982).

[2] P. Kumar and R.S. Bondurant, "Improving the Pulse Shape in Dye Laser Amplifiers: A New Technique," Appl. Opt. 22, 1284-1287 (May 1983).

[3] P. Kumar, R.S. Bondurant, J.H. Shapiro, and M.M. Salour, "Quantum Noise Measurements on Degenerate Four-Wave Mixing," in L. Mandel and E. Wolf (eds.) Coherence and Quantum Optics V (Plenum, New York, 1983) pp. 43-50.

[4] P. Kumar, J.H. Shapiro, and R.S. Bondurant, "Fluctuations in the Phase-Conjugate Signal Generated via Degenerate Four-Wave Mixing," Opt. Commun. 50, 183-188 (June 1984).

[5] R.S. Bondurant, P. Kumar, J.H. Shapiro, and M. Maeda, "Degenerate Four-Wave Mixing as a Possible Source of Squeezed-State Light," Phys. Rev. A 30, 343-353 (July 1984).

[6] R.S. Bondurant, M. Maeda, P. Kumar, and J.H. Shapiro, "Pump and Loss Effects on Degenerate Four-Wave Mixing Quantum Statistics," in L. Mandel and E. Wolf (eds.), Coherence and Quantum Optics V, (Plenum, New York, 1983), pp. 767-774.

[7] P. Kumar and J.H. Shapiro, "Squeezed State Generation via Forward Degenerate Four-Wave Mixing," submitted to Phys. Rev. A., preprint attached as Appendix I.

[8] J.H. Shapiro, "Quantum Noise and Excess Noise in Optical Homodyne and Heterodyne Receivers," submitted to IEEE J. Quantum. Electron., preprint attached as Appendix II.

[9] J.H. Shapiro and S.S. Wagner, "Phase and Amplitude Uncertainties in Heterodyne Detection," IEEE J. Quantum Electron. QE-20, 803-813 (July 1984).

[10] J.H. Shapiro, "Near Optimum and Optimum Receiver Realizations for Binary Two-Photon Coherent State Signals," Presented at the 1983 IEEE International Symposium on Inform. Theory, St. Jovite, Canada.

[11] R.S. Bondurant and J.H. Shapiro, "Squeezed States in Phase-Sensing Interferometers," in L. Mandel and E. Wolf (eds.), Coherence and Quantum Optics V (Plenum, New York, 1983), pp. 629-636.

[12] R.S. Bondurant and J.H. Shapiro, "Squeezed States in Phase-Sensing Interferometers," submitted to Phys. Rev. D.

[13] H.P. Yuen and J.H. Shapiro, "Generation and Detection of Two-Photon Coherent States via Degenerate Four-Wave Mixing," Opt. Lett. 4 334-336 (October 1979).

[14] R.J. Cook, "Photon Dynamics," Phys. Rev. A. 25, 2164-2167 (April 1982).

[15] H.P. Yuen and J.H. Shapiro, "Optical Communication with Two-Photon Coherent States - Part III: Quantum Measurements Realizable with Photoemissive Detectors," IEEE Trans. Inform. Theory IT-26, 78-92 (January 1980).

[16] H.P. Yuen and V.W.S. Chan, "Noise in Homodyne and Heterodyne Detection," Opt. Lett. 8, 177-179 (March 1983); errata, Opt. Lett. 8 345 (June 1983).

[17] C.W. Helstrom, "Detection Theory and Quantum Mechanics," Inform. Contr. 10, 254-291 (March 1967).

[18] C.W. Helstrom, Quantum Detection and Estimation Theory (Academic, New York, 1976) Chap. 4.

[19] R.S. Kennedy, "A Near-Optimum Receiver for the Binary Coherent State Quantum Channel," MIT Res. Lab. Electron. Quart. Prog. Rep. 108, 219-225 (January 1973).

[20] S.J. Dolinar, "An Optimum Receiver for the Binary Coherent State Quantum Channel," MIT Res. Lab. Electron. Quart. Prog. Rep. 111, 115-120 October 1973).

[21] J.H. Shapiro, "On the Near-Optimum Binary Coherent-State Receiver," IEEE Trans. Inform. Theory IT-26, 490-491 (July 1980).

[22] C.M. Caves, "Quantum Mechanical Noise in an Interferometer," Phys. Rev. D, 23, 1693-1708 (April 1981).

[23] H.P. Yuen, "Contractive States and the Standard Quantum Limit for Monitoring Free Mass Positions," Phys. Rev. Lett. 51, 719-722 (August 1983).

PERSONNEL

The research reported here was carried out by

Prof. Jeffrey H. Shapiro, principal investigator

Dr. Prem Kumar, research scientist

Dr. Roy S. Bondurant, research assistant

Ms. Mari W. Maeda, research assistant

Mr. Stuart S. Wagner, graduate student

Mr. Josef Ocenasek, graduate student

Mr. Ben P. Wise, undergraduate student

PUBLICATIONS

The following publications have been produced under this research effort.

1. R.S. Bondurant, P. Kumar, J.H. Shapiro, and M.M. Salour, "Photon Counting Statistics of Pulsed Light Sources," Opt. Lett. 7, 529-531 (November 1982).
2. J.H. Shapiro, "Mysteries and Applications of Two-Photon Coherent States," presented at Lasers '82, New Orleans, LA, 1982.
3. S.S. Wagner, "An Investigation of the Uncertainties in Signal Energy and Phase in Optical Detection," S.M. thesis, Dept. of Elect. Eng. and Comput. Sci., MIT (September 1982).
4. B.P. Wise, "Cross Entropy Probability Estimation," S.B. thesis, Dept. of Physics, MIT (June 1982).
5. P. Kumar and R.S. Bondurant, "Improving the Pulse Shape in Dye Laser Amplifiers: A New Technique," Appl. Opt. 22, 1284-1287 (May 1983).
6. P. Kumar, R.S. Bondurant, J.H. Shapiro, and M.M. Salour, "Quantum Noise Measurements on Degenerate Four-Wave Mixing," in L. Mandel and E. Wolf (eds.) Coherence and Quantum Optics V (Plenum, New York, 1983) pp. 43-50.
7. R.S. Bondurant, M. Maeda, P. Kumar, and J.H. Shapiro, "Pump and Loss Effects on Degenerate Four-Wave Mixing Quantum Statistics," in L. Mandel and E. Wolf (eds.), Coherence and Quantum Optics V, (Plenum, New York, 1983), pp. 767-774.
8. R.S. Bondurant and J.H. Shapiro, "Squeezed States in Phase-Sensing Interferometers," in L. Mandel and E. Wolf (eds.), Coherence and Quantum Optics V (Plenum, New York, 1983), pp. 629-636.
9. J.H. Shapiro, "Near Optimum and Optimum Receiver Realizations for Binary Two-Photon Coherent State Signals," Presented at the 1983 IEEE International Symposium on Inform. Theory, St. Jovite, Canada.

10. J.H. Shapiro, "Mysteries and Applications of Two-Photon Coherent States," presented at the Workshop on New Directions in Phase-Conjugate Nonlinear Optics, Los Alamos NM, 1983.

11. R.S. Bondurant, "Theoretical and Experimental Aspects of Quantum Noise Reduction and Precision Measurements," Ph.D. thesis, Dept. of Elect. Eng. and Comput. Sci., MIT (July 1983).

12. J. Ocenasek, "The Performance of an Optical Waveguide Tap Using a Multimode Directional Coupler," S.M. thesis, Dept. of Elect. Eng. and Comput. Sci., MIT (August 1983).

13. R.S. Bondurant, P. Kumar, J.H. Shapiro, and M. Maeda, "Degenerate Four-Wave Mixing as a Possible Source of Squeezed-State Light," Phys. Rev. A 30, 343-353 (July 1984).

14. P. Kumar, J.H. Shapiro, and R.S. Bondurant, "Fluctuations in the Phase-Conjugate Signal Generated via Degenerate Four-Wave Mixing," Opt. Commun. 50, 183-188 (June 1984).

15. J.H. Shapiro, P. Kumar, M.W. Maeda, and R.S. Bondurant, "Quantum Noise and the Detection of Squeezed States," J. Opt. Soc. Am. B 1, 517-518 (June 1984).

16. P. Kumar and J.H. Shapiro, "Squeezed State Generation via Forward Degenerate Four-Wave Mixing," submitted to Phys. Rev. A., preprint attached as Appendix I.

17. R.S. Bondurant and J.H. Shapiro, "Squeezed States in Phase-Sensing Interferometers," submitted to Phys. Rev. D.

18. J.H. Shapiro, "Quantum Noise and Excess Noise in Optical Homodyne and Heterodyne Receivers," submitted to IEEE J. Quantum. Electron., preprint attached as Appendix II.

19. P. Kumar, "Degenerate Four-Wave Mixing Lineshapes in Sodium Vapor Under Pulsed Excitation," to be submitted to Opt. Lett., preprint attached as Appendix III.

APPENDIX I

SQUEEZED STATE GENERATION VIA FORWARD DEGENERATE FOUR WAVE MIXING

Prem Kumar and Jeffrey H. Shapiro

Research Laboratory of Electronics

Massachusetts Institute of Technology

Cambridge, MA 02139

ABSTRACT

Degenerate four wave mixing (DFWM) has been suggested as a possible generation scheme for squeezed state light. A recent analysis of the quantum effects of probe-conjugate loss in backward DFWM has shown that such loss puts an absolute limit on the squeezing that can be obtained via this generation scheme. In this communication we show that it is the counter-propagating beam geometry of backward DFWM that makes it ill suited for squeezed state generation. On the other hand, the nominally copropagating beam geometry of forward DFWM is shown to alleviate the absolute probe-conjugate loss limit on squeezing.

PACS Headings: 42.50. + q, 42.65. - k, 05.30. -d

I. Introduction

Degenerate four wave mixing (DFWM) has been suggested by Yuen and Shapiro as a possible source for squeezed state generation[1]. Their model was a simple extension of the classical description of DFWM given by Yariv and Pepper[2]. Quantizing only the probe and the signal beams while retaining classical descriptions for the pump beams and the nonlinear medium, they showed that a two-photon coherent state (TCS) (essentially a minimum uncertainty squeezed state) is obtained by a 50/50 combination of the phase conjugate reflected beam and the transmitted probe beam from backward DFWM. A recent analysis by Bondurant, Maeda, Kumar and Shapiro has shown that probe-conjugate loss puts an absolute limit on the squeezing that can be obtained via backward DFWM[3]. Since then Reid and Walls have given a fully quantum mechanical treatment of backward DFWM[4]. Their analysis neglected the spatial propagation effects and showed that pump induced spontaneous emission limits the amount of squeezing achievable. In this communication we show that the absolute limit on probe-conjugate loss is because the preceding work all addressed backward DFWM, which has a counter-propagating beam geometry. This geometry is ideal for correcting phase aberrations via conjugate-wave generation, but is ill-suited for squeezed state generation because of the afore-mentioned probe-conjugate loss limit. We show that forward DFWM, which has a nominally copropagating nonplanar beam geometry, removes the absolute probe-conjugate loss limit. Such an interaction geometry has been applied recently in studies of pressure induced four wave mixing interactions[5].

In section II we start with a classical analysis of forward DFWM. It is well known that large nonlinearities are obtained when the operating frequency is chosen near an atomic or molecular resonance. Therefore, in section III, we develop a semi-classical treatment of forward DFWM in an atomic medium consisting of an ensemble of stationary two-level atoms. In section IV we quantize

the electromagnetic fields and examine the squeezing behavior of the output beams.

II. Classical Equations

Consider the geometry shown in fig. 1. Two weak waves of wavevectors $\bar{k}_1$ and $\bar{k}_2$ propagate at small angles $\pm \phi/2$ from the z direction, determining a plane P. The pump waves of wavevectors $\bar{k}_3$ and $\bar{k}_4$ also nominally propagate along the z direction; $\bar{k}_3$ and $\bar{k}_4$ are obtained from $\bar{k}_1$ and $\bar{k}_2$ by rotating the plane P along the CC' axis. With this choice of wavevectors we note that $\bar{k}_1 + \bar{k}_2 = \bar{k}_3 + \bar{k}_4$, i.e., the phase matching condition is satisfied.

The fields are taken to be co-polarized[6] plane waves of angular frequency ω

$$E_j(\bar{r},t) = \frac{1}{2} A_j(r_j)\exp[i(\omega t - \bar{k}_j \cdot \bar{r})] + \text{c.c.} \tag{1}$$

where r_j denotes the distance measured along $\bar{k}_j$. Following Yariv and Pepper[2] we can derive the following equations for coupled modes 1 and 2

$$\frac{dA_1}{dz} = -i\kappa^* A_2^*, \qquad \frac{dA_2^*}{dz} = i\kappa A_1, \tag{2}$$

where κ is the nonlinear coupling constant given by (mks units)

$$\kappa^* = \omega\chi^{(3)} A_3 A_4 / 2cn_o \cos\frac{\phi}{2}, \tag{3}$$

$\chi^{(3)}$ is the third order susceptibility of the nonlinear medium, c is the speed of light in vacuum and n_o is the background refractive index. Equation (2) has the following solution

$$A_1(z) = \cosh(|\kappa|z)\, A_1(0) - i\frac{\kappa^*}{|\kappa|}\sinh(|\kappa|z)\, A_2^*(0), \tag{4a}$$

$$A_2^*(z) = \cosh(|\kappa|z)\, A_2^*(0) + i\frac{\kappa}{|\kappa|}\sinh(|\kappa|z)\, A_1(0), \tag{4b}$$

in terms of boundary conditions at z = 0.

III. Collisionless Two Level Medium

We now consider an ensemble of stationary two level atoms forming the nonlinear medium. The atoms are characterized by a dipole moment, μ, and longitudinal and transverse relaxation times T_1 and T_2 respectively. Following Abrams and Lind[7] we obtain the following equations for the coupled modes 1 and 2

$$\frac{dA_1}{dz} = -\gamma A_1 - i\kappa^* A_2^*, \quad \frac{dA_2^*}{dz} = -\gamma A_2^* + i\kappa A_1 , \tag{5}$$

where

$$\gamma = \frac{2\alpha_0}{n} \frac{\omega}{\omega_0} \frac{(1+\delta^2)}{\left(1+\delta^2+\frac{|A_3|^2+|A_4|^2}{A_s^2}\right)^2} \frac{1}{\cos(\phi/2)} \tag{6}$$

and

$$\kappa^* = \frac{2\alpha_0}{n} \frac{\omega}{\omega_0} \frac{(\delta+i)}{\left(1+\delta^2+\frac{|A_3|^2+|A_4|^2}{A_s^2}\right)^2} \frac{2A_3A_4}{A_s^2\cos(\phi/2)} , \tag{7}$$

$\delta = (\omega-\omega_0)T_2$ is the normalized detuning from line center, $A_s^2 = \hbar^2/T_1T_2\mu^2$ is proportional to the line-center saturation intensity, ω_0 is the atomic transition frequency, $\alpha_0 = \mu^2\Delta N_0 T_2\omega_0/2\varepsilon_0 c\hbar$ is the line-center small-signal-field attenuation coefficient, $\Delta N_0 = (N_1-N_2)$ is the equilibrium population difference in the absence of the applied fields, n is the saturated refractive index given by

$$k^2 = \frac{\omega^2}{c^2}\left(n_o^2 - \frac{2\alpha_o c}{\omega_o}\ \frac{\delta(1+\delta^2)}{\left(1+\delta^2 + \frac{|A_3|^2 + |A_4|^2}{A_s^2}\right)^2}\right) \equiv \frac{n_\omega^2 \omega^2}{c^2}\ , \tag{8}$$

and k is the magnitude of the propagation vectors in the medium. We note that the pumps are nominally copropagating, so that no spatial averaging along the pump direction is required. Such averaging drastically reduces the DFWM reflectivity in the conventional counter-propagating pumps geometry[7].

Equation (5) yields the following solution,

$$A_1(z) = e^{-\gamma z}\left[\cosh(|\kappa|z)\ A_1(0) - i\ \frac{\kappa^*}{|\kappa|}\ \sinh(|\kappa|z)\ A_2^*(0)\right] \tag{9a}$$

$$A_2^*(z) = e^{-\gamma z}\left[i\ \frac{\kappa}{|\kappa|}\ \sinh(|\kappa|z)\ A_1(0) + \cosh(|\kappa|z)\ A_2^*(0)\right], \tag{9b}$$

in terms of boundary conditions at z = 0.

IV. Squeezed State Generation

A. Lossless Case

In giving a quantum treatment of backward DFWM, Yuen and Shapiro[1] replace the complex field amplitudes A_j and A_j^* with the photon annihilation and creation operators a_j and $a_j^\dagger$, respectively, for j = 1,2. They assume that the pump fields A_3 and A_4 are strong and hence can be treated classically. They also describe the medium by a classical third order susceptibility. Using their approach for our forward DFWM geometry we replace Eq. (2) with

$$\frac{da_1}{dz} = -i\kappa^* a_2^\dagger\ , \quad \frac{da_2^\dagger}{dz} = i\kappa a_1 \tag{10}$$

which has the following solution for a z=0 to z=L interaction

$$a_1(L) = \mu a_1(0) - i\nu a_2^\dagger(0) \tag{11a}$$

$$a_2^\dagger(L) = \mu a_2^\dagger(0) + i\nu^* a_1(0). \tag{11b}$$

Here $\mu = \cosh(|\kappa|L)$, $\nu = e^{-i\Theta}\sinh(|\kappa|L)$, $\kappa = |\kappa|e^{i\Theta}$, $a_1(0)$ and $a_2(0)$ are the input field operators at $z = 0$. The outputs at $z = L$ are combined through a 50/50 beam splitter to generate two new modes described by annihilation operators c and d such that

$$c = [a_1(L) - ia_2(L)]/2^{1/2} \tag{12a}$$

$$d = [a_1(L) + ia_2(L)]/2^{1/2}, \tag{12b}$$

in terms of which the solutions become

$$c = \mu c_{in} - \nu c_{in}^\dagger, \quad d = \mu d_{in} + \nu d_{in}^\dagger \tag{13}$$

where $c_{in} = [a_1(0) - ia_2(0)]/2^{1/2}$ (14a)

$$d_{in} = [a_1(0) + ia_2(0)]/2^{1/2} \tag{14b}$$

are annihilation operators describing field modes obtained by linear combination of the input modes to the four-wave mixer. Because $|\mu|^2-|\nu|^2=1$, it follows that c and d are in TCS if $a_1(0)$ and $a_2(0)$ are in coherent states (CS).[8]

B. DFWM in a lossy medium

It was shown in section IV A that modes c and d are in TCS. Let us concentrate on the quadrature noise behavior of mode c. Let $c_1 = \frac{c+c^\dagger}{2}$ and $c_2 = \frac{c-c^\dagger}{2i}$ be the in-phase and out-of-phase quadratures of mode c, respectively. Then from Eq. (13) one can show that the quadrature variances are

$$\langle \Delta c_1^2 \rangle \equiv \langle (c_1 - \langle c_1 \rangle)^2 \rangle = |\mu-\nu|^2/4 \tag{15a}$$

$$\langle \Delta c_2^2 \rangle \equiv \langle (c_2 - \langle c_2 \rangle)^2 \rangle = |\mu+\nu|^2/4, \tag{15b}$$

when $a_1(0)$ and $a_2(0)$ are in CS[8]. Thus arbitrarily large squeezing is obtained in c_1 when $|\nu|$ is made arbitrarily large with $\mu\nu^*$ real and positive. Large values of $|\nu|$ have been shown to be obtainable in resonant media, such as described in section III[9]. An inspection of Eqs. (6), (7) together with the defining equations for μ and ν shows that a large value of $|\nu|$ is necessarily accompanied by a large value of γ, the loss per unit length in the medium. We follow the approach of Bondurant et al.[3] to analyze the effect of this probe-conjugate loss on the squeezing obtainable via forward DFWM in a resonant medium.

We note that Eq. (10) can be obtained from the effective interaction Hamiltonian

$$H_I = \hbar v(\kappa a_1 a_2 + \kappa^* a_2^\dagger a_1^\dagger) \tag{16}$$

using the Heisenberg equations of motion and then converting the temporal differential equations into spatial differential equations by the change of variable $z = vt$.

In order to account for probe-conjugate loss quantum mechanically we adjoin the system of Eq. (16) to two reservoirs of loss oscillators[10] described by annihilation operators b_ℓ^s, for $\ell = 1$ to ∞ and $s = 1,2$. The total effective interaction Hamiltonian can therefore be written as

$$H_I^T = \hbar v[\kappa a_1 a_2 + \kappa^* a_2^\dagger a_1^\dagger] + \hbar \sum_{s=1}^{2} [a_s \sum_{\ell=1}^{\infty} \kappa_\ell^* b_\ell^{s\dagger} + a_s^\dagger \sum_{\ell=1}^{\infty} \kappa_\ell b_\ell^s], \tag{17}$$

where κ_ℓ represents the coupling between the modes of interest, i.e., a_1 and a_2, and the loss oscillator modes. From Eq. (17), we obtain two coupled spatial differential equations for the slowly-varying operators a_1 and a_2

$$\frac{da_1}{dz} = -\gamma a_1 - i\kappa^* a_2^\dagger + G_1(z) \tag{18a}$$

$$\frac{da_2^\dagger}{dz} = -\gamma a_2^\dagger + i\kappa a_1 + G_2^\dagger(z) \tag{18b}$$

where γ is the loss per unit length and $G_s(z)$, $s = 1,2$ are Langevin noise operators obeying

$$\gamma a_s(z) = v^{-2} \sum_\ell |\kappa_\ell|^2 \int_0^z a_s(z')\exp[i(\omega_\ell-\omega)(z'-z)/v]\, dz', \quad s=1,2, \tag{19a}$$

and

$$G_s(z) = -\frac{i}{v} \sum_\ell \kappa_\ell b_\ell^s(0)\exp[i(\omega-\omega_\ell)z/v]; \quad s=1,2 \tag{19b}$$

respectively. These noise operators, under the Wigner-Weisskopf approximation, obey the commutation rule

$$[G_s(z), G_{s'}^\dagger(z')] = 2\gamma\, \delta_{ss'}\delta(z-z') \text{ for } s, s'=1,2. \tag{20}$$

The set of equations (18) can be integrated with the result

$$a_1(L) = e^{-\gamma L}[\mu a_1(0) - i\nu a_2^\dagger(0)] + \Gamma_1 \tag{21a}$$

$$a_2^\dagger(L) = e^{-\gamma L}[i\nu a_1^*(0) + \mu a_2^\dagger(0)] + \Gamma_2^\dagger \tag{21b}$$

where

$$\Gamma_1 = \int_0^L e^{-\gamma(L-z')}[\cosh(|\kappa|(L-z'))G_1(z') - ie^{-i\Theta}\sinh(|\kappa|(L-z'))G_2^\dagger(z')]dz' \tag{22a}$$

$$\Gamma_2 = \int_0^L e^{-\gamma(L-z')}[-ie^{-i\Theta}\sinh(|\kappa|(L-z'))G_1^\dagger(z') + \cosh(|\kappa|(L-z'))G_2(z')]dz'. \tag{22b}$$

The loss per unit length, γ, appearing in Eq. (19a) is numerically the same as that in Eq. (6) for a medium consisting of stationary two level atoms.

Operator equation (21) reduces to the classical equation (5) when expectation values are taken.

To calculate the effect of probe-conjugate loss on squeezing, we construct new modes as in Eq. (12) and evaluate the quadrature variances. As an example,

$$c = e^{-\gamma L}[\mu c_{in} - \nu c_{in}^{\dagger}] + (\Gamma_1 - i\Gamma_2)/2^{1/2} \tag{23}$$

and

$$\langle \Delta c_1^2 \rangle = \frac{e^{-2\gamma L}}{4}(\mu-\nu)^2 + \frac{1}{2}\langle (\Gamma_{11}+\Gamma_{22})^2 \rangle \; ; \tag{24}$$

where $\Gamma_{11} = (\Gamma_1+\Gamma_1^{\dagger})/2$, $\Gamma_{22} = (\Gamma_2-\Gamma_2^{\dagger})/2i$ and we have chosen pump phases such that $\Theta = 0$. After substituting Eqs. (22a) and (22b) into Eq. (24) and evaluating the appropriate moments, we get

$$\langle \Delta c_1^2 \rangle = \frac{\gamma(2N+1)}{4(\gamma+|\kappa|)} + \frac{1}{4}e^{-2(\gamma+|\kappa|)L}\left[1 - \frac{\gamma(2N+1)}{(\gamma+|\kappa|)}\right] \tag{25a}$$

and

$$\langle \Delta c_2^2 \rangle = \frac{\gamma(2N+1)}{4(\gamma-|\kappa|)} + \frac{1}{4}e^{-2(\gamma-|\kappa|)L}\left[1 - \frac{\gamma(2N+1)}{(\gamma-|\kappa|)}\right], \tag{25b}$$

where N measures the initial excitation of the reservoir modes, i.e., $N = \langle b_{\ell}^{s\dagger}(0)\, b_{\ell}^{s}(0)\rangle$, and is assumed to be the same for all the modes.

Several cases of interest can now be considered.

i) $\gamma=0$, i.e., the zero probe-conjugate loss limit, in which Eq. (25) reduces to Eq. (15) and ideal squeezing is obtained.

ii) $\gamma\neq 0, \gamma<|\kappa|$ and $L >> \frac{1}{|\gamma-|\kappa||}$. In this limit $\langle \Delta c_2^2 \rangle \to \infty$ and $\langle \Delta c_1^2 \rangle \to \frac{\gamma(2N+1)}{4(\gamma+|\kappa|)}$, i.e., for a given N ideal squeezing can be obtained by making $|\kappa| >> \gamma$. Though it should be noted that pump induced spontaneous emission noise will limit this squeezing as is the case in backward DFWM as shown in Ref. 4.

iii) $\gamma>|\kappa|$ and $L >> \frac{1}{(\gamma-|\kappa|)}$. In this limit $\langle \Delta c_1^2 \rangle \to \frac{\gamma(2N+1)}{4(\gamma+|\kappa|)}$ and $\langle \Delta c_2^2 \rangle \to \frac{\gamma(2N+1)}{4(\gamma-|\kappa|)}$. For N=0, i.e., when the loss oscillators are initially unexcited, we get $\langle \Delta c_1^2 \rangle = \frac{\gamma}{4(\gamma+|\kappa|)} \to 1/4$ and $\langle \Delta c_2^2 \rangle = \frac{\gamma}{4(\gamma-|\kappa|)} \to \frac{1}{4}$ for $\gamma>>|\kappa|$.

This result is expected here because loss totally dominates the nonlinear coupling and any quadrature noise asymmetry caused by the latter is swamped by the fluctuations introduced by the former. In the case of $\gamma=|\kappa|$, a squeezing factor of 2 is still obtained in $\langle\Delta c_1^2\rangle$. The uncertainty product $\langle\Delta c_1^2\rangle\langle\Delta c_2^2\rangle = (2N+1)^2/16(1-\frac{|\kappa|^2}{\gamma^2})> \frac{1}{16}$ implying that a squeezed state which is not a minimum uncertainty state is generated. Also, since for our choice of θ, $\mu\nu^*$ is real, this state is not a TCS either.[11]

V. Discussion

The results of the previous section show that the DFWM beam geometry plays an important role in determining the squeezing that can be obtained in a realistic experiment. The nonlinear coupling introduces quantum noise asymmetry between the quadratures of the interacting modes. In DFWM this asymmetry is between the quadratures of two different modes and mode mixing at the output of the DFWM interaction is required to obtain new modes, whose two quadratures show this asymmetry. *Probe-conjugate loss, on the other hand, introduces independent fluctuations into the two quadratures which are coupled via the non-linear interaction, thus tending to equalize the observed output beam quadrature fluctuations. The latter is the result of case (iii) in section IV, where loss dominates the nonlinear coupling.*

In the counterpropagating geometry of backward DFWM, the interaction at any point couples forward and backward going waves. Because of loss, each of these waves has suffered the noise-symmetrizing effect noted above. *It is the combination of the loss with the non-local nature (forward/backward wave coupling at all points in the interaction medium) that is responsible, we believe, for the severe loss-limit on backward DFWM squeezed-state generation.* On the other hand, in forward DFWM only forward going waves are coupled. Although loss injects a symmetric noise contribution at each point in the interaction medium, the nonlinear interaction from that point

to the end of the interaction squeezes that noise contribution. Thus, with the forward interaction and gain coefficient in excess of the loss coefficient, the only fundamental limit on achievable forward DFWM squeezing will be due to pump induced spontaneous emission. Indeed, our view of the physics of this problem is supported by Yuen's loss analysis for DPA squeezed state generation[8], which shows that in that forward-going three-wave interaction arbitrary squeezing is obtained for any γ and N so long as $|\kappa|$ can be made arbitrarily larger than γ.

In summary, forward DFWM appears more promising than backward DFWM as a squeezed state generator. It is a phase-matched interaction with no fundamental limit on squeezing due to probe-conjugate loss. Moreover, we expect there will be differences in the limits on obtainable squeezing set by pump-induced spontaneous emission in forward and backward DFWM, because of the different physics of their spatial propagation characteristics, as described above. Furthermore, since all the beams are propagating in roughly the same direction, the interaction is not velocity selective. The participation of all velocity groups results in a very large nonlinear interaction. Both experimental and theoretical investigations of forward DFWM have recently been published.[12] Phase conjugation and sub-Doppler resolution due to strong saturation have been reported.

The authors acknowledge helpful discussions with R.S. Bondurant and D.F. Walls. This work was supported by the Office of Naval Research Contract N00014-81-K-0662.

References

1. H.P. Yuen and J.H. Shapiro, Opt. Lett. 4, 334 (1979).

2. A. Yariv and D.M. Pepper, Opt. Lett. 1, 16 (1977).

3. R.S. Bondurant, M. Maeda, P. Kumar and J.H. Shapiro in "Coherence and Quantum Optics, V," eds. L. Mandel and E. Wolf, pp. 767-774, Plenum Press, NY, 1983; R.S. Bondurant, P. Kumar, J.H. Shapiro and M. Maeda, submitted to Phys. Rev. A.

4. M.D. Reid and D.F. Walls, submitted to Optics Communications.

5. Y. Prior, Appl. Opt. 19, 1741 (1980); J.A. Shirley, R.J. Hall, and A.C. Eckbreth, Opt. Lett. 5, 380 (1980); A.R. Bogdan, Y. Prior, and N. Bloembergen, Opt. Lett. 6, 82 (1981); Y. Prior, A.R. Bogdan, M. Dagenais, and N. Bloembergen, Phys. Rev. Lett. 46, 111 (1981).

6. We assume the polarization to be perpendicular to plane P and ignore the complicating effects due to a small angle ϕ between the electric field vectors of the pumps and $\phi/2$ between the electric field vector of the pump and the probe.

7. R.L. Abrams and R.C. Lind, Opt. Lett. 2, 94, (1978); 3, 205 (1978).

8. H.P. Yuen, Phys. Rev. A 13, 2226 (1976).

9. R.C. Lind and D.G. Steel, Opt. Lett. 6, 554 (1981).

10. W.H. Louisell, "Quantum Statistical Properties of Radiation," Wiley, New York, 1973.

11. H.P. Yuen, Phys. Lett. 56A, 105 (1976).

12. Y. Prior and E. Yarkoni, Phys. Rev. A 28, 3689 (1983); A. Khyzniak, V. Kondilenko, Yu. Kucherov, S. Lensik, S. Odoulov, and M. Soskin, J. Opt. Soc. Am. A 1, 169 (1984).

Figure Captions

1. Forward DFWM geometry.

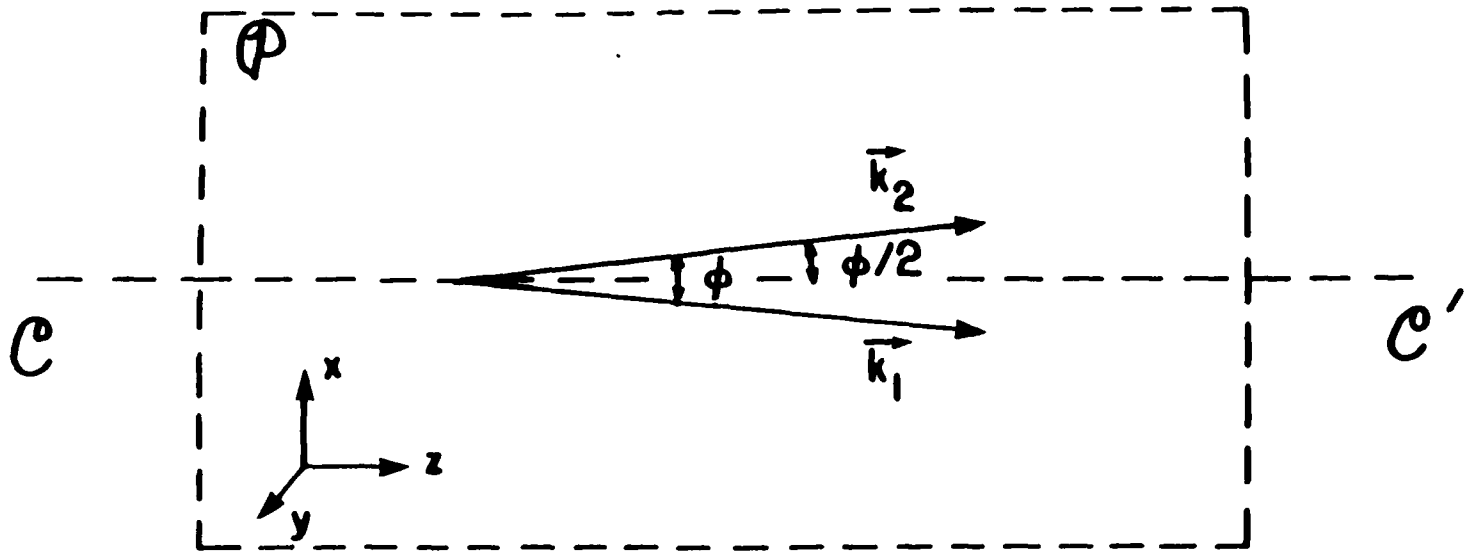

igure 1

QUEEZED STATE GENERATION ...

em Kumar et al.,

APPENDIX II

QUANTUM NOISE AND EXCESS NOISE IN OPTICAL HOMODYNE AND HETERODYNE RECEIVERS

Jeffrey H. Shapiro

Department of Electrical Engineering and Computer Science
and Research Laboratory of Electronics
Massachusetts Institute of Technology
Cambridge, MA 02139

Abstract

A parallel development of the semiclassical and quantum statistics of multi-spatiotemporal mode direct, homodyne, and heterodyne detection using an ideal (except for its sub-unity quantum efficiency) photon detector is presented. Particular emphasis is placed on the latter two coherent detection configurations. The primary intent is to delineate the semiclassical theory's regime of validity and to show, within this regime of validity, how the quantum theory's signal quantum noise, local oscillator quantum noise, the quantum noise incurred because of sub-unity detector quantum efficiency, plus (for heterodyning only) image band quantum noise produce the quantitative equivalent of the semiclassical theory's local oscillator shot noise. The effects of classical fluctuations on the local oscillator, and the recently suggested dual-detector arrangement for suppressing these fluctuations, are treated. It is shown that previous studies of this arrangement have neglected a potentially significant noise contribution.

I. INTRODUCTION

In coherent optical detection [1] - [3], the optical field to be measured is combined on the surface of a photodetector with the field of a strong local oscillator laser whose center frequency is offset by an amount $\Delta\nu$ from that of the signal field. The detection scheme is referred to as optical homodyning if $\Delta\nu=0$, and optical heterodyning if $\Delta\nu=\nu_{IF}>0$, with ν_{IF} being the intermediate frequency in the latter case. For both schemes, electrical filtering of the photocurrent is used to select the beat frequency components in the vicinity of $\Delta\nu$, yielding an output that contains a frequency translated replica of the signal field components that were coherent in space and time with the local oscillator field. Heterodyne detection is now widely employed in coherent CO_2 laser radars [4], [5], and is being vigorously researched for use with semiconductor injection lasers in fiber optics [6] - [8] and space communications [9], [10]. Performance analyses in these areas routinely employ the semiclassical statistical model for photodetection, which implies that the fluctuations observed in coherent optical detection with signal and local oscillator fields of perfect amplitude and frequency stability comprise an additive white Gaussian noise, representing local oscillator shot noise.

It has long been known [11] that the semiclassical statistics for photodetection are quantum mechanically correct only when the total field illuminating the detector is in a Glauber coherent state or a classically random mixture of such states. Inasmuch as ordinary light sources, including lasers and light emitting diodes, obey this classical state condition, there is no need to abandon the semiclassical approach in the vast majority of photodetection sensitivity calculations. However, non-classical light has been generated via resonance fluorescence, as confirmed by observations of its photon anti-bunching [12] and sub-Poissonian behavior [13] in direct detection. Moreover, there is great

theoretical interest in squeezed states (also called two-photon coherent states) [14], [15], which are non-classical states of considerable potential for optical communications [16] - [19] and precision measurements [20] - [23]. For these states, the quantum theory of photodetection is essential, and coherent optical detection schemes are the most interesting.

In [18], Yuen and Shapiro developed the quantum descriptions of single-detector optical homodyne and heterodyne receivers. They employed a quasimonochromatic approximation, and assumed a coherent state local oscillator, corresponding to perfect local oscillator amplitude and frequency stability. Within these limitations, complete statistics for multi-spatiotemporal mode detection are available from [18]. More recently [22], the fact that photodetectors respond to photon flux rather than power [24] has been used to relax somewhat the quasimonochromatic approximation in [18]. Thus, were high power, highly stable local oscillator lasers available at all wavelengths of interest, the quantum photodetection theory of [18] would provide a sufficiently general foundation for all optical homodyne and heterodyne sensitivity calculations. Unfortunately, such is not the case.

Driven by heterodyne-detection problems arising from the excess noise of semiconductor injection lasers, Yuen and Chan [25] proposed a dual-detector arrangement for coherent optical detection, akin to the balanced mixer concept of microwave technology [26], [27]. They gave a direct quantum analysis of single-mode dual-detector homodyning, showing that local oscillator quantum and excess noises can be balanced out, hence alleviating injection laser problems that would have plagued a single-detector system. In subsequent work by Chan and his collaborators, the basic dual-detector excess noise cancellation concept was demonstrated experimentally [28], and a variety of non-ideal device effects (quantum efficiency mismatch, etc.) were analyzed using semiclassical multi-temporal mode

techniques [29]. Also, Schumaker [30] has shown that the dual-detector single-mode homodyne arrangement is better than single-detector homodyning for making non-classical squeezed state observations, as a result of its ability to cancel out local oscillator excess noise.

Because the quantum treatments in [25] and [30] are confined to single-mode situations, and the multi-mode results in [28], [29] are in essence semiclassical, there is as yet no fully quantum treatment of multi-mode dual-detector coherent optical reception. This paper will develop such a model by generalizing the results of [18]. Simple explicit representations for all of the relevant output terms in coherent optical detection with a strong but classically random local oscillator field will be derived. It will be seen that the previous dual-detector analyses [25], [28] - [30] neglect excess-noise modulation of the signal and quantum noise terms, and the first of these modulation effects may significantly degrade output signal-to-noise ratio in some circumstances. Moreover, because of the calculational power afforded by [18], our rather general quantum results are more directly comparable with those of the multi-mode semiclassical theory than are the more limited results of [25], [30]. Indeed, that comparison is the primary purpose of this paper.

The paper's core, Section II, is a parallel development of the semiclassical and quantum statistics of multi-spatiotemporal mode direct, homodyne, and heterodyne detection using an ideal (except for its sub-unity quantum efficiency) photon detector. The formulation therein for the coherent optical detection schemes will assume perfectly stable local oscillators in the semiclassical models, and the corresponding coherent state local oscillators in the quantum models. We use Section II to delineate the semiclassical theory's regime of validity, and to show, within this regime, how the combination of the quantum theory's signal quantum noise, local oscillator quantum noise, the quantum noise incurred because of

sub-unity detector quantum efficiency, plus (for heterodyning only) image band quantum noise produce the quantitative equivalent of the semiclassical theory's local oscillator shot noise. In Section III we address coherent optical detection with classically random local oscillators. The technique of iterated expectation is used to readily obtain both semiclassical and quantum results for this case. Single-detector and dual-detector systems are considered, and our results are compared, in the case of dual-detector quantum homodyning to those of [25], [30]. Finally, in Section IV we briefly discuss the implications of our work for squeezed state generation experiments, which is the application that motivated our analysis.

II. SEMICLASSICAL VS. QUANTUM PHOTODETECTION

The central element of all the photodetection configurations we will consider is shown in Fig. 1. It is a surface photoemitter with active region $\bar{x} = (x,y) \in A_d$ in the z=0 plane, illuminated by a quasimonochronomatic (center frequency ν_0) paraxial scalar electromagnetic wave from the half space z<0 over an observation time interval $t \in T$. This detector is assumed to have a constant quantum efficiency η over the frequency band containing the illuminating field. The output of the detector is a scalar current density $J(\bar{x},t)$ for $\bar{x} \in A_d$, $t \in T$. As will be described below, the field characterization we must employ for the illumination is either classical or quantum mechanical, according to whether semiclassical or quantum photodetection statistics are sought. Although we shall neglect internal time constant and noise effects, which are present in real detectors, our direct detection results will be applicable to photomultiplier tubes (for which the current gain permits internal noise to be overcome) at post-detection bandwidths up to the reciprocal anode response time of the tube. Furthermore, our results will be applicable to coherent optical detection systems using semiconductor photodiodes (for which the mixing gain overcomes the internal noise) up to the post-detection bandwidth of the detector. No particular loss of

generality is entailed by the use of scalar rather than vector fields, with the caveat that all the coherent optical detection work herein presumes that the actual signal and local oscillator fields are co-polarized. Finally, by appropriate spatial integrations, we can collapse our current density observation to photocurrent observations for a single detector or a multiple-detector array.

A. Direct Detection

In direct detection, the electromagnetic field to be measured comprises the entire illumination, and the basic observation quantity is the current density $J(\bar{x},t)$.

Semiclassical Model Let $E^{(+)}(\bar{x},t)$ be the positive-frequency complex field (V/m units) associated with the classical scalar electric field incident on the detector, i.e., $E^{(+)}(\bar{x},t)$ is the analytic signal of this electric field. Because of our quasimonochromatic assumption, the Fourier transform [1] of $E^{(+)}$

$$E^{(+)}(\bar{x},\nu) = \int dt\ E^{(+)}(\bar{x},t)\ e^{j2\pi\nu t} \tag{1}$$

is non-zero only for $|\nu - \nu_0| \leq B$, where the bandwidth B is much less than the center frequency ν_0. Because of our paraxial assumption, the short time average power density falling on the point $\bar{x}$ at time t is

$$I(\bar{x},t) = (c\varepsilon_0/2)\ E^{(-)}(\bar{x},t)E^{(+)}(\bar{x},t), \tag{2}$$

where c is the speed of light, ε_0 the permittivity of free space, and $E^{(-)} \equiv (E^{(+)})^*$ is the negative-frequency complex field, with * denoting complex conjugate.

The standard semiclassical photodetection model [31], in our notation, presumes that $J(\bar{x},t)$ is a conditional space-time Poisson impulse train with rate function $\lambda(\bar{x},t) = RI(\bar{x},t)/e$ where e is the electron charge, and R is the detector's responsivity (A/W units) at the illumination's center frequency ν_0. This means that:

1) the current density, which is of the form

$$J(\bar{x},t) = \sum_n e\delta(\bar{x}-\bar{x}_n)\delta(t-t_n), \tag{3}$$

has shot effect noise, i.e., it consists of instantaneous emissions of an electron charge e at the random space-time points $\{(\bar{x}_n,t_n) : \bar{x}_n \varepsilon A_d,\ t_n \varepsilon T\}$;

2) conditioned on knowledge of the rate function $\{\mu(\bar{x},t) : \bar{x}\varepsilon A_d, t\varepsilon T\}$, the number of photoemissions occurring within a spatial region $A' \subseteq A_d$ during a time interval $T' \subseteq T$ is a Poisson random variable with mean value $\int_{A'} d\bar{x}' \int_{T'} dt\ \mu(\bar{x},t)$;

3) conditioned on knowledge of $\{\mu(\bar{x},t) : \bar{x}\varepsilon A_d\ ,\ t\varepsilon T\}$, the photoemissions occurring in disjoint spaial regions $A', A'' \subset A_d$ are statistically independent processes,

4) conditioned on knowledge of $\{\mu(\bar{x},t): \bar{x}\varepsilon A_d, t\varepsilon T\}$, the photoemissions occurring in disjoint time intervals $T', T'' \subset T$ are statistically independent processes.

Even though the semiclassical theory of photodetection employs classical fields, it is customary to recognize in this theory that light of frequency ν is quantized into photons of energy $h\nu$, where h is Planck's constant. Thus, for the quasimonochromatic case at hand, the responsivity is ordinarily written as $R = e\eta/h\nu_0$, in terms of the detector's quantum efficiency η and the photon energy at the field's center frequency, so that $\mu(\bar{x},t) = \eta I(\bar{x},t)/h\nu_0$. In fact, because we are concerned with detectors that, quantum mechanically, respond to photon-flux density rather than power density [24], [22], it is more proper to write

$$\mu(\bar{x},t) = \eta I_{ph}(\bar{x},t), \tag{4}$$

where I_{ph} is the classical photon-flux density

$$I_{ph}(\bar{x},t) = E^{*}(\bar{x},t)E(\bar{x},t) \tag{5}$$

obtained from the $(\text{photons/s})^{1/2}/\text{m}$ units positive-frequency complex field

$$E(\bar{x},t) = \int d\nu(c\varepsilon_0/2h\nu)^{1/2} E^{(+)}(\bar{x},\nu)e^{-j2\pi\nu t}. \tag{6}$$

For all practical purposes in the semiclassical theory, with quasimonochromatic light we can use $\mu(\bar{x},t) = \eta I(\bar{x},t)/h\nu_0$ and $\mu(\bar{x},t) = \eta I_{ph}(\bar{x},t)$ interchangeably. This amounts to using $\nu \doteq \nu_0$ in the square-root term of (6), an approximation whose validity is guaranteed by (1). In the quantum theory, even with quasimonochromatic light, it is critical to employ the photon-flux density formulation, see [22].

Quantum Model In the quantum photodetection theory, the classical positive-frequency complex field $E^{(+)}(\bar{x},t)$ is replaced by a positive-frequency field operator $\hat{E}^{(+)}(\bar{x},t)$, whose quantum state is specified by a density operator ρ. The quasimonochromatic and paraxial conditions of the semiclassical theory become conditions on the density operator, namely, that the excited (non-vacuum state) modes of $\hat{E}^{(+)}(\bar{x},t)$ lie at frequencies within B of ν_0 and propagate at small angles to the z axis. As in [17], [18], [22], we shall regard the current density $J(\bar{x},t)$ as a classical quantity, corresponding to the macroscopic output[2] of the quantum measurement performed by the detector of Fig. 1 on the field $\hat{E}^{(+)}(\bar{x},t)$. To provide an explicit representation of this quantum measurement, we must first develop the quantum effective photon-flux density.

Let us convert $\hat{E}^{(+)}(\bar{x},t)$ to a photon-units field operator by defining

(cf. Eqs. (1), (6))

$$\hat{E}^{(+)}(\bar{x},\nu) = \int dt\, \hat{E}^{(+)}(\bar{x},t)\, e^{j2\pi\nu t}\,, \tag{7}$$

and

$$\hat{E}(\bar{x},t) = \int d\nu\, (c\varepsilon_0/2h\nu)^{1/2}\, \hat{E}^{(+)}(\bar{x},\nu) e^{-j2\pi\nu t}\,. \tag{8}$$

Equation (8) defines the same basic field operator used in [16] - [18], [22]. We can made a modal expansion

$$\hat{E}(\bar{x},t) = \sum_n \hat{a}_n \xi_n(\bar{x},t), \quad \bar{x}\varepsilon A_d,\ t\varepsilon T \tag{9}$$

of this operator, where $\{\hat{a}_n\}$ are modal annihilation operators satisfying the commutation rules

$$[\hat{a}_n,\hat{a}_m] = 0, \quad [\hat{a}_n,\hat{a}_m^{+}] = \delta_{nm}, \tag{10}$$

and $\{\xi_n\}$ are a complete orthonormal set of classical functions over $\bar{x}\varepsilon A_d$, $t\varepsilon T$. In Eq. (10), the $\{\hat{a}_n^{+}\}$ are the adjoints of the $\{\hat{a}_n\}$; they are modal creation operators.

For a detector of sub-unity quantum efficiency we must adjoin to (9) a fictitious field

$$\hat{E}_{vac}(\bar{x},t) = \sum_n \hat{c}_n \xi_n(\bar{x},t), \quad \bar{x}\varepsilon A_d,\ t\varepsilon T, \tag{11}$$

where $\{\hat{c}_n\}$ are modal annihilation operators that commute with $\{\hat{a}_n\}$ and $\{\hat{a}_n^{+}\}$, viz.

$$[\hat{c}_n,\hat{c}_m] = [\hat{c}_n,\hat{a}_m] = [\hat{c}_n,\hat{a}_m^{\dagger}] = 0 ,$$
$$[\hat{c}_n,\hat{c}_m^{\dagger}] = \delta_{nm}. \tag{12}$$

The fields $\hat{E}$ and $\hat{E}_{vac}$ are quantum-mechanically independent, with the latter having all its modes in the vacuum state. In terms of $\hat{E}$ and $\hat{E}_{vac}$, the effective photon-flux density operator for the detector is

$$\hat{I}'_{ph}(\bar{x},t) = \hat{E}'^{\dagger}(\bar{x},t)\hat{E}'(\bar{x},t) , \tag{13}$$

with

$$\hat{E}'(\bar{x},t) \equiv \eta^{1/2}\hat{E}(\bar{x},t) + (1-\eta)^{1/2}\hat{E}_{vac}(\bar{x},t) . \tag{14}$$

The representation theorem of quantum photodetection [18, theorem 1] can now be stated (in our notation) as follows. The classical current density $J(\bar{x},t)$ obtained from photoemissive detection measures the quantum operator

$$\hat{J}(\bar{x},t) = e\hat{I}'_{ph}(\bar{x},t) , \tag{15}$$

i.e., it is proportional to the effective photon-flux density. In somewhat more detail this means (cf. the semiclassical case):

1) the current density obeys

$$J(\bar{x},t) = \sum_n e\,\delta(\bar{x}-\bar{x}_n)\delta(t-t_n) , \tag{16}$$

so it is still a collection of instantaneous emissions of an electron charge at random space-time points $\{(\bar{x}_n,t_n)\}$;

2) if $F(J(\bar{x},t))$ is an arbitrary functional of the current density, then the classical average of this random variable $\langle F(J(\bar{x},t))\rangle$ equals the quantum average $\mathrm{tr}(\rho' F(\hat{J}(\bar{x},t)))$, where tr denotes trace and $\rho' = \rho \otimes \rho_{vac}$ gives the joint density operator for $\hat{E}$ and $\hat{E}_{vac}$ in terms of the density operator ρ for $\hat{E}$ and the vacuum-state density operator $\rho_{vac} = \bigotimes_n |0\rangle\langle 0|$ for $\hat{E}_{vac}$.

Note that we cannot dispense with the vacuum state field $\hat{E}_{vac}$ unless $n=1$, even though its average value obeys $\mathrm{tr}(\rho_{vac}\, \hat{E}_{vac}(\bar{x},t)) = 0$ regardless of the value of n. This is because the zero-point fluctuations (vacuum-state quantum noise) in $\hat{E}_{vac}$ can contribute to $F(J(\bar{x},t))$. Indeed the noise in $J(\bar{x},t)$ has nothing to do with the snot effect associated with the discreteness of the electron charge. Rather, it is the quantum noise in $\hat{E}'$ being observed through measurement of the effective photon-flux density.

Comparison Let us suppose that the density operator for $\hat{E}$ is a classical state[3], i.e.,

$$\rho = \int d^2\underset{\sim}{\alpha}\, P(\underset{\sim}{\alpha};\underset{\sim}{\alpha}^*)\, |\underset{\sim}{\alpha}\rangle\langle\underset{\sim}{\alpha}| \tag{17}$$

with

$$\hat{a}_n |\underset{\sim}{\alpha}\rangle = \alpha_n |\underset{\sim}{\alpha}\rangle \tag{18}$$

defining the multi-mode Glauber coherent states of the field $\hat{E}$ in terms of the modal expansion (9), and $P(\underset{\sim}{\alpha};\underset{\sim}{\alpha}^*)$ being a classical probability density function $P(\underset{\sim}{\alpha};\underset{\sim}{\alpha}^*) \geq 0$, $\int d^2\underset{\sim}{\alpha}\, P(\underset{\sim}{\alpha};\underset{\sim}{\alpha}^*) = 1$. It was shown in [18] that this is a necessary and sufficient condition for the semiclassical statistics to be

quantitatively correct. In particular, under this condition the quantum model predicts that $J(\bar{x},t)$ is a conditional space-time Poisson impulse train with conditional rate function

$$\mu(\bar{x},t) = \eta E^*(\bar{x},t)E(\bar{x},t) \tag{19}$$

for

$$E(\bar{x},t) \equiv \sum_n \alpha_n \xi_n(\bar{x},t) = \langle \underset{\sim}{\alpha} | \hat{E}(\bar{x},t) | \underset{\sim}{\alpha} \rangle \ . \tag{20}$$

the average field illuminating the detector given the state of $\hat{E}$ is the multi-mode coherent state $|\underset{\sim}{\alpha}\rangle$.

To illustrate the above behavior, let us examine the statistics of the observed photon count[4]

$$N = e^{-1} \int_{A_d} d\bar{x} \int_T dt \ J(\bar{x},t) \tag{21}$$

assuming single-mode illumination, and $\eta = 1$. In the semiclassical theory we shall take

$$E(\bar{x},t) = [\alpha/(A_d T)^{1/2}] e^{-j2\pi\nu_0 t}, \ \bar{x}\varepsilon A_d, t\varepsilon T \ , \tag{22}$$

where α is a complex-valued random variable with probability density function $p(\alpha)$, A_d is the area of A_d, and T is the duration of T. We then obtain Mandel's rule [32] for the probability distribution of N

$$Pr[N = n] = \int d^2\alpha \ p(\alpha) \ (|\alpha|^{2n}/n!) \exp(-|\alpha|^2) \ , \tag{23}$$

viz. N is a conditionally Poisson random variable. Equation (23) gives the mean and variance of the observed photocount to be

$$\langle N \rangle = \int d^2\alpha \; p(\alpha) \; |\alpha|^2 \; = \; \langle |\alpha|^2 \rangle \tag{24}$$

and

$$\text{var}(N) = \langle N \rangle + \text{var}\,(|\alpha|^2), \tag{25}$$

respectively, where the first term on the right in (25) represents shot noise and the second term on the right in (25) represents excess noise.

In the quantum theory we let $\xi_1(\overline{x},t) = (A_d T)^{-1/2} e^{-j2\pi\nu_o t}$ be the only excited mode in (9), so that the density operator for $\hat{E}$ is

$$\rho = \rho_1 \underset{n>1}{\otimes} |0\rangle\langle 0| \tag{26}$$

for ρ_1 the density operator of mode 1. We then find for the probability distribution of N [11], [17]

$$Pr[N = n] \; = \; \langle n|\rho_1|n\rangle \; , \tag{27}$$

where

$$\hat{a}_1^{+}\hat{a}_1|n\rangle = n|n\rangle \tag{28}$$

defines the photon number states of the first mode of $\hat{E}$. If ρ_1 is the classical state.

$$\rho_1 = \int d^2\alpha \; p(\alpha) \quad |\alpha\rangle\langle\alpha| \quad , \tag{29}$$

with $p(\alpha)$ being the probability density from the semiclassical theory

(cf. Eq. (17)), then (27) reduces to (23) as expected. Thus, in this case the semiclassical theory is quantitatively correct in its prediction of the photon counting probability distribution. It is nevertheless physically incorrect, in that it ascribes the photon counting fluctuations to shot noise, whereas they are actually a manifestation of the illumination field's quantum noise. For example, were $\rho_1 = |k><k|$ where $|k>$ is the k-photon number state (a non-classical state), then we would get

$$Pr[N=n] = \delta_{nk} \tag{30}$$

from (27), whence

$$<N> = k \ , \tag{31}$$

and

$$var(N) = 0 \ , \tag{32}$$

for the photon count mean and variance. Here the field state is an eigenket of our observation operator, so there is no uncertainty in the measurement outcome. This sub-Poissonian behavior cannot be obtained from the semiclassical theory, because for all $p(\alpha)$ the excess noise term in (25) will be non-negative, forcing $var(N) \geq <N>$ to prevail.

B. Homodyne Detection

The configuration we shall consider for single-detector multi-spatiotemporal mode homodyne detection is shown in Fig. 2. The signal field to be detected is combined, through a lossless beam splitter of intensity transmission ε, with a perfectly stable local oscillator field on the surface of the Fig. 1 photodetector. The resulting current density, $J_{hom}(\bar{x},t)$, is our homodyne detection output, whose statistics we shall characterize below. By spatial integration of our results over the detector's active region A_d, we can use our model to describe single-

detector homodyning; the extension to dual-detector homodyning will be made in Section III.

Semiclassical Model The total classical photon-units complex field incident on the photodetector is given by[5]

$$E(\bar{x},t) = \epsilon^{1/2}E_S(\bar{x},t) + (1-\epsilon)^{1/2}E_{LO}(\bar{x},t) \quad , \tag{33}$$

for $\bar{x}\epsilon A_d$, $t\epsilon T$, in terms of a (potentially random) weak signal field $E_S(\bar{x},t)$, and a deterministic strong local oscillator field $E_{LO}(\bar{x},t)$. The latter has a classical photon-flux density

$$I_{phLO}(\bar{x},t) = E_{LO}^{*}(\bar{x},t)E_{LO}(\bar{x},t) \quad , \tag{34}$$

that greatly exceeds that of the former

$$I_{phS}(\bar{x},t) = E_S^{*}(\bar{x},t)E_S(\bar{x},t) \quad , \tag{35}$$

for $\bar{x}\epsilon A_d, t\epsilon T$. Thus, the rate function driving the photodetector is, from (4), (5), (33)-(35), approximately

$$u(\bar{x},t) = \eta[(1-\epsilon)I_{phLO}(\bar{x},t)+2[\epsilon(1-\epsilon)]^{1/2}\mathrm{Re}(E_S(\bar{x},t)E_{LO}^{*}(\bar{x},t))] \quad . \tag{36}$$

It then follows, from the Central Limit Theorem for high density shot noise [33], [34], that at very large values of the local oscillator classical photon number

$$N_{phLO} = \int_{A_d} d\bar{x} \int_T dt \; I_{phLO}(\bar{x},t) \tag{37}$$

the homodyne detection current density $J_{hom}(\bar{x},t)$ is a conditional Gaussian process. Specifically, conditioned on knowledge of the signal field

$\{E_S(\bar{x},t) : \bar{x}\epsilon A_d,\ t\epsilon T\}$, $J_{hom}(\bar{x},t)$ is the sum of three current densities:

1) a homodyne-mixing current density signal term $2e\eta[\varepsilon(1-\varepsilon)]^{1/2}\mathrm{Re}(E_S(\bar{x},t)E_{LO}^{*}(\bar{x},t))$:

2) a direct-detection local oscillator bias current density $e\eta(1-\varepsilon)I_{phLO}(\bar{x},t)$; and

3) a local oscillator shot noise current density, which is a zero-mean spatiotemporal non-stationary white Gaussian noise process $J_{shot}(\bar{x},t)$ with covariance function

$$\langle J_{shot}(\bar{x}_1,t_1)J_{shot}(\bar{x}_2,t_2)\rangle = e^2\eta(1-\varepsilon)I_{phLO}(\bar{x}_1,t_1)\delta(\bar{x}_1-\bar{x}_2)\delta(t_1-t_2) \quad . \tag{38}$$

In order to connect the preceding multi-spatiotemporal mode formulation with more familiar single-detector multi-temporal mode results, let us consider the statistics of the single-detector homodyne photocurrent

$$i_{hom}(t) = \int_{A_d} d\bar{x}\ J_{hom}(\bar{x},t) \quad , \tag{39}$$

assuming that

$$E_{LO}(\bar{x},t) = (P_{LO}/h\nu_o A_d)^{1/2}\ e^{-j2\pi\nu_o t} \quad , \tag{40}$$

corresponding to a normally-incident plane wave local oscillator of power P_{LO}. Here we find that, conditioned on knowledge of the signal field, $i_{hom}(t)$ comprises a signal current

$$i_{sig}(t) = 2e\eta[P_{LO}\varepsilon(1-\varepsilon)/h\nu_o A_d]^{1/2}\mathrm{Re}\left(\int_{A_d} d\bar{x}\ E_S(\bar{x},t)e^{j2\pi\nu_o t}\right) , \tag{41}$$

plus a zero-frequency bias current

$$i_{bias} = e\eta(1-\epsilon)P_{LO}/h\nu_o \ , \tag{42}$$

plus a zero-mean stationary white Gaussian process shot-noise current $i_{shot}(t)$ with spectral density ei_{bias} (A^2/Hz) .

The signal current is a frequency-translated (to baseband) replica of the normally-incident plane wave component of $E_S(\bar{x},t)$ that is in phase with the local oscillator field. The bias current is the zero-frequency photocurrent produced by the local oscillator field. The noise current is the local-oscillator shot noise, whose spectrum follows the well known Schottky formula [35].

Quantum Model In the quantum model, Eq. (33) becomes an operator-valued expression

$$\hat{E}(\bar{x},t) = \epsilon^{1/2}\hat{E}_S(\bar{x},t) + (1-\epsilon)^{1/2}\hat{E}_{LO}(\bar{x},t), \tag{43}$$

giving the field operator $\hat{E}$ that drives the detector in terms of the signal field operator $\hat{E}_S$ and the local oscillator field operator $\hat{E}_{LO}$. The density operator ρ for $\hat{E}$ is assumed to be

$$\rho = \rho_S \otimes \rho_{LO} \tag{44}$$

where ρ_S is an arbitrary signal field density operator and $\rho_{LO} = |\underset{\sim}{\alpha}_{LO}\rangle\langle\underset{\sim}{\alpha}_{LO}|$ is a multi-mode coherent state local oscillator density operator. The latter corresponds to a mean local oscillator field

$$E_{LO}(\bar{x},t) \equiv \langle\underset{\sim}{\alpha}_{LO}|\hat{E}_{LO}(\bar{x},t)|\underset{\sim}{\alpha}_{LO}\rangle = \sum_n \alpha_{LOn}\,\xi_n(\bar{x},t) \ , \tag{45}$$

when $\hat{E}_{LO}$ is expanded using the mode set $\{\xi_n\}$ as was done for $\hat{E}$ in Eq. (9).

The strong local oscillator condition of the quantum theory,

$$\mathrm{tr}(\rho_S E_S^{+}(\bar{x},t)E_S(\bar{x},t)) \ll |E_{LO}(\bar{x},t)|^2 \quad , \tag{46}$$

is assumed to prevail (cf. Eqs. (34), (35)), with a very large average local oscillator photon number

$$N_{LO} \equiv \int_{A_d} d\bar{x} \int_T dt |E_{LO}(\bar{x},t)|^2 \gg 1, \tag{47}$$

(cf. Eq. (37)).

To obtain the effective photon-flux density operator measured by the detector we adjoin to $\hat{E}$ from (43) a quantum-mechanically independent vacuum-state field operator $\hat{E}_{vac}$, see Eqs. (11) - (14). We can now give a fully quantum characterization of the classical homodyne current density $J_{hom}(\bar{x},t)$, by translating the results of [18, theorem 2] into our notation. The strong local oscillator condition implies that this classical current density measures the quantum operator

$$\hat{J}_{hom}(\bar{x},t) = e\eta(1-\varepsilon)\hat{E}_{LO}^{+}(\bar{x},t)\hat{E}_{LO}(\bar{x},t) + 2e[\eta(1-\varepsilon)]^{1/2}\mathrm{Re}\{[(\eta\varepsilon)^{1/2}\hat{E}_S(\bar{x},t) + (1-\eta)^{1/2}\hat{E}_{vac}(\bar{x},t)] \cdot \hat{E}_{LO}^{+}(\bar{x},t)\} . \tag{48}$$

Moreover, because $N_{LO} \gg 1$, the local oscillator direct detection term in (48), $e\eta(1-\varepsilon)\hat{E}_{LO}^{+}(\bar{x},t)\hat{E}_{LO}(\bar{x},t)$, yields classical observation values comprising a bias current density $e\eta(1-\varepsilon)|E_{LO}(\bar{x},t)|^2$ plus a local oscillator quantum noise current density, which is a zero-mean spatiotemporal non-stationary white Gaussian noise process $J_{LOq}(\bar{x},t)$ with covariance function

$$\langle J_{LOq}(\bar{x}_1,t_1)J_{LOq}(\bar{x}_2,t_2)\rangle =$$

$$[e\eta(1-\varepsilon)]^2 E_{LO}(\bar{x}_1,t_1)^{*2}\delta(\bar{x}_1-\bar{x}_2)\delta(t_1-t_2) \tag{49}$$

Furthermore, under this same condition[6], the second term on the right in (48) simplifies to a homodyne-mixing signal operator $2e\eta[\varepsilon(1-\varepsilon)]^{1/2}\mathrm{Re}(\hat{E}_S(\bar{x},t)E_{LO}^*(\bar{x},t))$ plus a sub-unity quantum efficiency ($\eta<1$) quantum-noise current density. The latter current density is a zero-mean spatiotemporal non-stationary white Gaussian noise process $J_{vac}(\bar{x},t)$ with covariance function

$$\langle J_{vac}(\bar{x}_1,t_1)J_{vac}(\bar{x}_2,t_2)\rangle = e^2\eta(1-\eta)(1-\varepsilon)|E_{LO}(\bar{x}_1,t_1)|^2\delta(\bar{x}_1-\bar{x}_2)\delta(t_1-t_2)\ ; \tag{50}$$

J_{vac} is statistically independent of J_{LOq}. Thus, the classical homodyne current density $J_{hom}(\bar{x},t)$ measures the operator

$$\hat{J}_{hom}(\bar{x},t) = e\eta(1-\varepsilon)|E_{LO}(\bar{x},t)|^2 + J_{LOq}(\bar{x},t) + 2e\eta[\varepsilon(1-\varepsilon)]^{1/2}\,\mathrm{Re}(\hat{E}_S(\bar{x},t)E_{LO}^*(\bar{x},t)) + J_{vac}(\bar{x},t). \tag{51}$$

The first term on the right in (51) is the local oscillator bias current density, the second term is the classical representation of the local oscillator's quantum noise contributed by the $e\eta(1-\varepsilon)\hat{E}_{LO}^{\dagger}\hat{E}_{LO}$ measurement, and the last term is the classical representation of the $\eta<1$ quantum noise contributed by the $2e[\eta(1-\eta)(1-\varepsilon)]^{1/2}\mathrm{Re}(\hat{E}_{vac}(\bar{x},t)E_{LO}^*(\bar{x},t))$ measurement. The signal field contribution to $\hat{J}_{hom}(\bar{x},t)$ cannot be simplified further without knowledge of the density operator ρ_S. In general, this term will contribute signal field quantum noise to the homodyne observation, as will be seen below.

Comparison To facilitate comparison of the semiclassical and the quantum theories of homodyning, we shall restrict our consideration to the single detector case. First, we need the quantum characterization of the homodyne photocurrent (39), which can be obtained by spatial integration of the results just presented. We assume a normally-incident plane wave mean local oscillator field

$$E_{LO}(\bar{x},t) = (P_{LO}/h\nu_o A_d)^{1/2} e^{-j2\pi\nu_o t} , \quad (52)$$

and we find the $i_{hom}(t)$ measures the operator

$$\hat{i}_{hom}(t) = i_{bias} + i_{LOq}(t) + 2e\eta[P_{LO}\varepsilon(1-\varepsilon)/h\nu_o A_d]^{1/2} \mathrm{Re}\left(\int_{A_d} d\bar{x}\hat{E}_S(\bar{x},t)\, e^{j2\pi\nu_o t}\right) + i_{vac}(t) . \quad (53)$$

Here, i_{bias} is given by (42), and i_{LOq} and i_{vac} are statistically independent zero-mean stationary white Gaussian noise processes with spectral densities $e\eta(1-\varepsilon)i_{bias}$ and $e(1-\eta)i_{bias}$, respectively.

Physically, i_{bias} is the local oscillator bias current, i_{LOq} is the local oscillator quantum-noise current, and i_{vac} is the $\eta<1$ quantum-noise current. Equation (53) differs from the semiclassical description in two respects: the homodyne-mixing signal term involves the quantum field operator $\hat{E}_S$ rather than the classical field E_S ; the noise in the homodyne observation is a combination of local oscillator quantum noise, $\eta<1$ quantum noise, and signal quantum noise, rather than simply being local oscillator shot noise. We know, from the direct detection discussion, that the semiclassical photodetection model is quantitatively correct if the density operator ρ for the field $\hat{E}$ illuminating the detector represents a classical state. This situation occurs, under (44), if and only if ρ_S ,the signal field density operator, is a classical state

$$\rho_S = \int d^2\underline{\alpha}_S P_S(\underline{\alpha}_S;\underline{\alpha}_S^*)|\underline{\alpha}_S><\underline{\alpha}_S| \quad (54)$$

for $|\underline{\alpha}_S>$ the multi-mode signal field coherent state in modal expansion of $\hat{E}_S$ similar to Eq. (9), with P_S being a classical probability density. When (54) applies, the homodyne-mixing signal term in (53) can be given a classical representation akin to that employed for the $\hat{E}_{vac}$ mixing term in going from

(48) to (51). In particular, for a classical signal field state, the quantum theory of homodyning predicts that

$$i_{hom}(t) = i_{bias} + i_{LOq}(t) + 2en[P_{LO}\varepsilon(1-\varepsilon)/h\nu_o A_d]^{1/2}\mathrm{Re}\left(\int_{A_d} d\bar{x}E_S(\bar{x},t)\, e^{j2\pi\nu_o t}\right) + i_{Sq}(t) + i_{vac}(t) \quad , \tag{55}$$

where

$$E_S(\bar{x},t) \equiv \langle \underline{\alpha}_S | \hat{E}_S(\bar{x},t) | \underline{\alpha}_S \rangle \tag{56}$$

is the classical mean signal field when the state of $\hat{E}_S$ is $|\underline{\alpha}_S\rangle$. and $i_{Sq}(t)$ is a zero-mean stationary white Gaussian noise current of spectral density $en\varepsilon i_{bias}$ that is statistically independent of i_{LOq} and i_{vac}. The classical field E_S is, in general, a random process with probability density $P_S(\underline{\alpha}_S;\underline{\alpha}_S^*)$ in modal expansion form. The current $i_{Sq}(t)$ is the classical representation of the coherent state signal field quantum noise as observed through the measurement operator (53). Note that

$$i'(t) \equiv i_{LOq}(t) + i_{Sq}(t) + i_{vac}(t) \tag{57}$$

is a zero-mean stationary white Gaussian noise process of spectral density ei_{bias} ,in quantitative agreement with the semiclassical $i_{shot}(t)$ result. Of course, the interpretation of the origin of the noise in homodyning is different in these two theories. Local oscillator shot noise is a semiclassical fiction; the noise seen in homodyne detection (with an ideal local oscillator) is local oscillator quantum noise, plus $\eta<1$ quantum noise, plus signal quantum

noise. Moreover, in the limit $\eta\varepsilon \to 1$ with $\eta(1-\varepsilon)N_{LO} >> 1$, the two former contributions disappear, and homodyning gives a direct quantum measurement of the signal field component that is coherent in space and in phase with the local oscillator [18]. It is this characteristic that makes homodyning attractive for squeezed state applications [16] - [19].

C. Heterodyne Detection

The configuration for single-detector multi-spatiotemporal mode heterodyne detection, shown in Fig. 3, mimics that employed for homodyne detection. The only differences are that the signal field is centered at frequency $\nu_o + \nu_{IF}$, the local oscillator is centered at frequency ν_o, and passband filtering of the current density is used to select beat frequency components in the vicinity of the IF frequency ν_{IF} ($\nu_{IF}T>>1$ will be assumed). The bandwidth B of the signal field will be taken to be much less than ν_{IF}, and we shall concern ourselves with characterizing the statistics of the current density $J_{het}(\bar{x},t)$. The results we need are easily developed by injecting the frequency offset ν_{IF} into the preceding homodyne work.

Semiclassical Model In Eq. (33) let us make the frequency offset of the signal field explicit by writing

$$E_S(\bar{x},t) = F_S(\bar{x},t)e^{-j2\pi(\nu_o+\nu_{IF})t} \quad , \tag{58}$$

where F_S is a baseband complex signal field of bandwidth B. The results following (37) now provide the semiclassical statistics for heterodyning, namely, conditioned on knowledge of the baseband signal field $\{F_S(\bar{x},t) : \bar{x}\varepsilon A_d, t\varepsilon T\}$, $J_{het}(\bar{x},t)$ is the sum of three current densities:

1) a heterodyne-mixing current density signal term

$$2e\eta[\varepsilon(1-\varepsilon)]^{1/2}\mathrm{Re}(F_S(\bar{x},t)e^{-j2\pi(\nu_o+\nu_{IF})t}E_{LO}{}^*(\bar{x},t)) \quad ;$$

2) a direct-detection local oscillator bias current density $en(1-\varepsilon)I_{phLO}(\bar{x},t)$; and

3) a local oscillator shot noise current density $J_{shot}(\bar{x},t)$ characterized by (38).

The single-detector heterodyne photocurrent

$$i_{het}(t) = \int_{A_d} d\bar{x}\, J_{het}(\bar{x},t) \quad , \tag{59}$$

assuming E_{LO} is given by (40), then comprises a signal current

$$i_{sig}(t)=2en[P_{LO}\varepsilon(1-\varepsilon)/\, h\nu_o A_d]^{1/2}Re\left(\int_{A_d} d\bar{x}F_S(\bar{x},t)e^{-j2\pi\nu_{IF}t}\right) \quad , \tag{60}$$

plus a bias current i_{bias} from (42), plus a zero-mean stationary white Gaussian process shot-noise current $i_{shot}(t)$ with spectral density ei_{bias}.

The heterodyne current (59) is thus a frequency translated (from $\nu_o+\nu_{IF}$ to ν_{IF}) version of the normally incident plane wave component of E_S plus the usual bias and shot noise terms. Because of the frequency offset ν_{IF} between the signal and the local oscillator fields, both the in-phase and quadrature (relative to the local oscillator) components of the signal field contribute to the output observations.

Quantum Model Here we suppose that the only non-vacuum state modes of the field operator $\hat{E}_S$ lie within a bandwidth B of the frequency $\nu_o+\nu_{IF}$. However, because of zero-point fluctuations, the quantum version of (58) is

$$\hat{E}_S(\bar{x},t) = \hat{F}_S(\bar{x},t)e^{-j2\pi(\nu_o+\nu_{IF})t} + \hat{F}_I(\bar{x},t)e^{-j2\pi(\nu_o-\nu_{IF})t} \quad , \tag{61}$$

where $\hat{F}_S$ and $\hat{F}_I$ are baseband complex signal and image field operators. Physically, the image band, being ν_{IF} Hz below the local oscillator's frequency, contributes quantum noise to J_{het} even when it is unexcited [18], [22]. We shall assume that $\hat{F}_S$ and $\hat{F}_I$ are quantum-mechanically independent, with

the latter having all its modes in the vacuum state[7]. We now find, from the quantum homodyning work, that $J_{het}(\bar{x},t)$ measures the operator

$$\hat{J}_{het}(\bar{x},t) = en(1-\varepsilon)|E_{LO}(\bar{x},t)|^2 + J_{LOq}(\bar{x},t)$$

$$+ \ 2en[\varepsilon(1-\varepsilon)]^{1/2}\mathrm{Re}(\hat{F}_S(\bar{x},t)e^{-j2\pi(\nu_o+\nu_{IF})t}E_{LO}^*(\bar{x},t))$$

$$+2en[\varepsilon(1-\varepsilon)]^{1/2}\mathrm{Re}(\hat{F}_I(\bar{x},t)e^{-j2\pi(\nu_o-\nu_{IF})t}E_{LO}^*(\bar{x},t)] \ + \ J_{vac}(\bar{x},t) \ , \quad (62)$$

where E_{LO}, J_{LOq}, and J_{vac} are as given in (51). We can use the vacuum-state nature of $\hat{F}_I$ to obtain the classical representation

$$2en[\varepsilon(1-\varepsilon)]^{1/2}\mathrm{Re}(\hat{F}_I(\bar{x},t)e^{-j2\pi(\nu_o-\nu_{IF})t}E_{LO}^*(\bar{x},t))$$

$$= J_{Iq}(\bar{x},t)/2^{1/2} \ , \quad (63)$$

where J_{Iq} is a zero-mean non-stationary white Gaussian classical process corresponding to the image-band quantum noise, with covariance function

$$\langle J_{Iq}(\bar{x}_1,t_1)J_{Iq}(\bar{x}_2,t_2)\rangle =$$

$$(en)^2\varepsilon(1-\varepsilon)|E_{LO}(\bar{x}_1,t_1)|^2\delta(\bar{x}_1-\bar{x}_2)\delta(t_1-t_2) \ . \quad (64)$$

Thus, the quantum description of the single-detector heterodyne photocurrent $i_{het}(t)$ from (59) is that it measures the operator

$$i_{het}(t) = i_{bias} + i_{LOq}(t) + i_{Iq}(t)/2^{1/2} + i_{vac}(t)$$

$$+ \ 2en[P_{LO}\varepsilon(1-\varepsilon)/h\nu_o A_d]^{1/2}\mathrm{Re}\left(\int_{A_d} d\bar{x}\hat{F}_S(\bar{x},t)e^{-j2\pi\nu_{IF}t}\right) \ , \quad (65)$$

where i_{bias} , i_{LOq} , and $i_{vac}(t)$ are as in (53) and $i_{Iq}(t)$ is a zero mean white Gaussian noise process (the classical representation of image-band quantum noise) of spectral height $en\epsilon i_{bias}$.

Comparison Suppose the density operator for $\hat{F}_S$ is a classical state, i.e., its density operator ρ_{F_S} obeys

$$\rho_{F_S} = \int d^2\underline{\alpha}_S \, P_{F_S}(\underline{\alpha}_S;\underline{\alpha}_S^*) \; |\underline{\alpha}_S><\underline{\alpha}_S| \; , \tag{66}$$

where P_{F_S} is a classical probability density, and $|\underline{\alpha}_S>$ is the multi-mode Glauber coherent state for the modal expansion

$$\hat{F}_S(\bar{x},t) = \sum_n{}' \hat{a}_{Sn} \xi_n(\bar{x},t) e^{j2\pi(\nu_o+\nu_{IF})t} \; , \tag{67}$$

with $\sum_n{}'$ denoting summation over modes ξ_n lieing within bandwidth B of frequency $\nu_o+\nu_{IF}$. Here we can obtain a classical representation of the $\hat{F}_S$ term in (65) which reduces the quantum description of the heterodyne photocurrent to

$$\begin{aligned} i_{het}(t) &= i_{bias} + i_{LOq}(t) + i_{Iq}(t)/2^{1/2} + i_{vac}(t) \\ &+ 2en[P_{LO}\varepsilon(1-\varepsilon)/h\nu_o A_d]^{1/2} \mathrm{Re}\left(\int_{A_d} d\bar{x} \, F_S(\bar{x},t) e^{-j2\pi\nu_{IF}t} \right) \\ &+ i_{Sq}(t)/2^{1/2} \; , \end{aligned} \tag{68}$$

where the total noise current, $i_{LOq} + i_{Iq}/2^{1/2} + i_{Sq}/2^{1/2} + i_{vac}$,

is a zero-mean white Gaussian process with spectral density ei_{bias}, in quantitative agreement with the semiclassical theory, and

$$F_S(\bar{x},t) \equiv \langle \underline{\alpha}_S | \hat{F}_S(\bar{x},t) | \underline{\alpha}_S \rangle \tag{69}$$

is the classical baseband signal field envelope $\hat{F}_S$ associates with the coherent state $|\underline{\alpha}_S\rangle$. Note that half of the $\hat{E}_S$ quantum noise entering i_{het} comes through the signal field operator $\hat{F}_S$ and the other half comes through the image field operator $\hat{F}_I$.[8]

III. EXCESS NOISE EFFECTS AND DUAL-DETECTOR OPERATION

In this section we shall extend the results of Section II for coherent optical reception to include classical excess noise on the local oscillator field and dual-detector operation. It is convenient to begin with a presentation of dual-detector results in the absence of excess noise.

A. Dual-Detector Coherent Optical Reception

Suppose the homodyne/heterodyne configurations of Figs. 2 and 3 are augmented by the use of another quantum efficiency η detector on the previously unused output port of their beam splitters, see Fig. 4. We take the classical output field for this port to be

$$E(\bar{x},t) = -(1-\varepsilon)^{1/2} E_S(\bar{x},t) + \varepsilon^{1/2} E_{LO}(\bar{x},t) \tag{70}$$

in the semiclassical model, and use the corresponding operator-valued expression in the quantum model. Rather than treat the full multi-spatiotemporal mode situation, we shall restrict our attention to the photocurrents $i_1(t)$ and $i_2(t)$ obtained by spatial integration of the current densities $J_1(\bar{x},t)$ and $J_2(\bar{x},t)$ produced by detectors 1 and 2. We shall assume a perfectly stable (i.e, deterministic) classical local oscillator field

$$E_{LO}(\bar{x},t) = F_{LO}(\bar{x},t)e^{-j2\pi\nu_o t} \tag{71}$$

with baseband complex envelope F_{LO} in the semiclassical model, and a Glauber coherent state quantum local oscillator with mean field

$$tr(\rho_{LO}\hat{E}_{LO}(\bar{x},t)) = F_{LO}(\bar{x},t)e^{-j2\pi\nu_o t} \tag{72}$$

with baseband complex envelope F_{LO} in the quantum model. Under these conditions the results of Section II can be used to show that the following statistics apply.

Homodyne Detection In homodyning, the signal field is centered on ν_o, so, because of (71),(72), it is convenient to introduce baseband signal complex envelopes via

$$E_S(\bar{x},t) = F_S(\bar{x},t)e^{-j2\pi\nu_o t} \tag{73}$$

and

$$\hat{E}_S(\bar{x},t) = \hat{F}_S(\bar{x},t)e^{-j2\pi\nu_o t} \quad , \tag{74}$$

for the semiclassical and quantum cases, respectively. Now we have, semiclassically, that

$$\begin{aligned} i_1(t) = {} & en(1-\varepsilon)\int_{A_d} d\bar{x}|F_{LO}(\bar{x},t)|^2 \\ & + 2en[\varepsilon(1-\varepsilon)]^{1/2}\mathrm{Re}\left(\int_{A_d} d\bar{x}F_S(\bar{x},t)\ F_{LO}{}^*(\bar{x},t)\right) \\ & + e[n(1-\varepsilon)\int_{A_d} d\bar{x}|F_{LO}(\bar{x},t)|^2]^{1/2}n_{shot1}(t), \end{aligned} \tag{75}$$

and

$$i_2(t) = e\eta\varepsilon\int_{A_d} d\bar{x}|F_{LO}(\bar{x},t)|^2$$
$$-2e\eta[\varepsilon(1-\varepsilon)]^{1/2}\mathrm{Re}\left(\int_{A_d} d\bar{x}\, F_S(\bar{x},t)F_{LO}^*(\bar{x},t)\right)$$
$$+e\left[\eta\varepsilon\int_{A_d} d\bar{x}|F_{LO}(\bar{x},t)|^2\right]^{1/2} n_{shot2}(t) \quad , \tag{76}$$

for the homodyne photocurrents, where $n_{shot1}(t)$ and $n_{shot2}(t)$ are statistically independent identically distributed zero-mean stationary white Gaussian noise processes of unity spectral density. Equations (75) and (76) have the usual bias plus mixing signal plus local-oscillator shot noise interpretation. Note that the beam splitter phase shift between the output ports forces the mixing signals to be 180^0 out of phase. Also, the independence of the local-oscillator shot noises follows because they are generated from deterministic illumination of two different detectors.

For the quantum case, we have that $\hat{i}_1(t)$ and $\hat{i}_2(t)$ measure the operators

$$\hat{i}_1(t) = e\eta(1-\varepsilon)\int_{A_d} d\bar{x}|F_{LO}(\bar{x},t)|^2$$
$$+ 2e\eta[\varepsilon(1-\varepsilon)]^{1/2}\mathrm{Re}\left(\int_{A_d} d\bar{x}\hat{F}_S(\bar{x},t)F_{LO}^*(\bar{x},t)\right)$$
$$+ e\eta(1-\varepsilon)\left[\int_{A_d} d\bar{x}|F_{LO}(\bar{x},t)|^2\right]^{1/2} n_{LOq}(t)$$
$$+ e\left[\eta(1-\eta)(1-\varepsilon)\int_{A_d} d\bar{x}|F_{LO}(\bar{x},t)|^2\right]^{1/2} n_{vac1}(t) \quad , \tag{77}$$

and

$$\hat{i}_2(t) = e\eta\varepsilon\int_{A_d} d\bar{x}|F_{LO}(x,t)|^2$$
$$-2e\eta[\varepsilon(1-\varepsilon)]^{1/2}\mathrm{Re}\left(\int_{A_d} d\bar{x}\, \hat{F}_S(\bar{x},t)F_{LO}^*(\bar{x},t)\right)$$

$$+en\varepsilon\left[\int_{A_d} d\bar{x}|F_{LO}(\bar{x},t)|^2\right]^{1/2} n_{LOq}(t)$$

$$+e\left[n(1-n)\varepsilon\int_{A_d} d\bar{x}|F_{LO}(\bar{x},t)|^2\right]^{1/2} n_{vac2}(t), \qquad (78)$$

where $n_{LOq}(t)$, $n_{vac1}(t)$, $n_{vac2}(t)$ are statistically independent identically distributed zero-mean stationary unity-spectrum Gaussian processes. The familiar bias plus quantum mixing signal plus local-oscillator quantum noise plus $n<1$ quantum noise interpretation applies to (77), (78). As in the semiclassical model, the mixing term appears 180^o out of phase in the two photocurrents. No such phase shift appears on the n_{LOq} term, as this noise arises out of the direct detection of $\hat{E}_{LO}$. Indeed, except for scale factors, the local-oscillator quantum noise contributions to $i_1(t)$ and $i_2(t)$ are completely correlated. The $n<1$ quantum noises are, on the other hand, statistically independent because they arise from different detectors. *Finally, when the signal field is in a classical state these quantum results can be shown to be in quantitative agreement with the foregoing semiclassical formulas.*

Heterodyne Detection For heterodyning we use (58), rather than (73), to introduce a baseband signal complex envelope for the semiclassical analysis. We then find that

$$i_1(t) = en(1-\varepsilon)\int_{A_d} d\bar{x}|F_{LO}(\bar{x},t)|^2$$

$$+2en[\varepsilon(1-\varepsilon)]^{1/2}\mathrm{Re}\left(\int_{A_d} d\bar{x}F_S(\bar{x},t)F_{LO}^*(\bar{x},t)e^{-j2\pi\nu_{IF}t}\right)$$

$$+e\left[n(1-\varepsilon)\int_{A_d} d\bar{x}|F_{LO}(\bar{x},t)|^2\right]^{1/2} n_{shot1}(t)\ , \qquad (79)$$

and

$$i_2(t) = e\eta\varepsilon\int_{A_d} d\bar{x}|F_{LO}(\bar{x},t)|^2$$
$$-2e\eta[\varepsilon(1-\varepsilon)]^{1/2}\mathrm{Re}\left(\int_{A_d} d\bar{x}F_S(\bar{x},t)F_{LO}^*(\bar{x},t)e^{-j2\pi\nu_{IF}t}\right)$$
$$+e[\eta\varepsilon\int_{A_d} d\bar{x}|F_{LO}(\bar{x},t)|^2]^{1/2}n_{shot2}(t), \qquad (80)$$

with interpretations as given following (75), (76). In the quantum case we use (61) instead of (74) and obtain the measurement operators

$$\hat{i}_1(t) = e\eta(1-\varepsilon)\int_{A_d} d\bar{x}|F_{LO}(\bar{x},t)|^2$$
$$+2e\eta[\varepsilon(1-\varepsilon)]^{1/2}\mathrm{Re}\left(\int_{A_d} d\bar{x}\hat{F}_S(\bar{x},t)F_{LO}^*(\bar{x},t)e^{-j2\pi\nu_{IF}t}\right)$$
$$+e\eta(1-\varepsilon)\left[\int_{A_d} d\bar{x}|F_{LO}(\bar{x}.t)|^2\right]^{1/2} n_{LOq}(t)$$
$$+e[\eta(1-\eta)(1-\varepsilon)\int_{A_d} d\bar{x}|F_{LO}(\bar{x},t)|^2]^{1/2}n_{vac1}(t)$$
$$+e\eta[\varepsilon(1-\varepsilon)2^{-1}\int_{A_d} d\bar{x}|F_{LO}(\bar{x},t)|^2]^{1/2}n_{Iq}(t) \quad , \qquad (81)$$

for detector 1 and

$$\hat{i}_2(t) = e\eta\varepsilon\int_{A_d} d\bar{x}|F_{LO}(\bar{x},t)|^2$$
$$-2e\eta[\varepsilon(1-\varepsilon)]^{1/2}\mathrm{Re}\left(\int_{A_d} d\bar{x}\hat{F}_S(\bar{x},t)F_{LO}^*(\bar{x},t)e^{-j2\pi\nu_{IF}t}\right)$$
$$+e\eta\varepsilon\left[\int_{A_d} d\bar{x}|F_{LO}(\bar{x},t)|^2\right]^{1/2}n_{LOq}(t)$$
$$+e[\eta(1-\eta)\varepsilon\int_{A_d} d\bar{x}|F_{LO}(\bar{x},t)|^2]^{1/2}n_{vac2}(t)$$
$$-e\eta[\varepsilon(1-\varepsilon)2^{-1}\int_{A_d} d\bar{x}|F_{LO}(\bar{x},t)|^2]^{1/2}n_{Iq}(t) \quad , \qquad (82)$$

for detector 2. In Eqs (81), (82) the interpretations and comments following (77), (78) are applicable. The noise $n_{Iq}(t)$, which represents image-band quantum noise, is another zero-mean stationary unity-spectrum white Gaussian process. It is statistically independent of $n_{LOq}(t)$ and $n_{vacj}(t)$ for $j = 1,2$, and appears with a sign reversal in $\hat{i}_1$ and $\hat{i}_2$ because it arises from the mixing term involving $\hat{F}_I$.

B. Local-Oscillator Excess Noise

The extension of the results of Section IIIA to incorporate classical excess noise on the local oscillator is extraordinarily simple, because of the form the preceding results have been cast in. Specifically, for the semiclassical theory we need only make the baseband local oscillator complex envelope F_{LO} in (71) a complex-valued random process with known statistics. Then the homodyne and heterodyne results of the semiclassical theory, namely Eqs. (75), (76) and Eqs. (79), (80), respectively, become conditional statistics assuming F_{LO} is known.[9] Unconditional statistics follow, via iterated expectation [38], from averaging over the local oscillator fluctuations, as will be illustrated below. In a similar manner, classical local-oscillator excess noise can be injected into the quantum model by making ρ_{LO} a classical-state density operator for which F_{LO}, the average baseband local-oscillator complex envelope given the local oscillator is known to be in the multi-mode coherent state $|\underline{\alpha}_{LO}\rangle$, is a complex-valued classical random process. The quantum homodyne and heterodyne results, Eqs. (77), (78), and (81), (82), respectively, are now conditional characterizations given F_{LO}. Unconditional statistics are again obtained by averaging over the local oscillator fluctuations.[10]

To illustrate our excess noise results, and compare them with relevant prior work [25], [28]-[30], we shall consider a single spatial mode/multi-temporal

mode local oscillator, for which F_{LO} in the semiclassical theory and $\hat{F}_{LO}$ in the quantum theory are both of the form $(P_{LO}(t)/h\nu_o A_d)^{1/2} \exp(-j\phi_{LO}(t))$, where $P_{LO}(t)$ and $\phi_{LO}(t)$ are classical random power and phase fluctuations. For convenience, we shall assume that these fluctuations are the polar decomposition of a stationary complex-Gaussian random process. We shall also assume that the signal field, in both the semiclassical and quantum pictures, is statistically independent of the local oscillator. Finally, we shall limit our consideration to the differenced output currents $i_1(t) - i_2(t)$.

Homodyne Detection Under the preceding conditions we have the semiclassical result

$$\begin{aligned} i_1(t) - i_2(t) &= e\eta(1-2\varepsilon)P_{LO}(t)/h\nu_o \\ &+4e\eta[\varepsilon(1-\varepsilon)P_{LO}(t)/h\nu_o A_d]^{1/2}\mathrm{Re}\left(\int_{A_d} d\bar{x}F_S(\bar{x},t)e^{j\phi_{LO}(t)}\right) \\ &+e[\eta(1-\varepsilon)P_{LO}(t)/h\nu_o]^{1/2}n_{shot1}(t) \\ &-e[\eta\varepsilon P_{LO}(t)/h\nu_o]^{1/2}n_{shot2}(t)\,, \end{aligned} \tag{83}$$

and the quantum result

$$\begin{aligned} \hat{i}_1(t) - \hat{i}_2(t) &= e\eta(1-2\varepsilon)P_{LO}(t)/h\nu_o \\ &+4e\eta[\varepsilon(1-\varepsilon)P_{LO}(t)/h\nu_o A_d]^{1/2}\mathrm{Re}\left(\int_{A_d} d\bar{x}\hat{F}_S(\bar{x},t)e^{j\phi_{LO}(t)}\right) \\ &+e\eta(1-2\varepsilon)(P_{LO}(t)/h\nu_o)^{1/2}n_{LOq}(t) \\ &+e[\eta(1-\eta)(1-\varepsilon)P_{LO}(t)/h\nu_o]^{1/2}n_{vac1}(t) \\ &-e[\eta(1-\eta)\varepsilon P_{LO}(t)/h\nu_o]^{1/2}\,n_{vac2}(t)\,. \end{aligned} \tag{84}$$

In both (83) and (84), the first term on the right equals a mean bias current $e\eta(1-2\varepsilon)\langle P_{LO}(t)\rangle/h\nu_o$ plus a local oscillator power-fluctuation excess noise $e\eta(1-2\varepsilon)(P_{LO}(t)-\langle P_{LO}(t)\rangle)/h\nu_o$. Both of these are exactly nulled when the beam splitter is 50/50, i.e., when $\varepsilon = 1/2$. The second term on the right in (83) and (84) is the homodyne-mixing signal current; local oscillator randomness both amplitude and phase modulates this term. The remaining terms in the semiclassical result (83) are the shot noises, now modulated by local oscillator power fluctuations. The remaining terms in the quantum result are the local oscillator quantum noise and the $\eta<1$ quantum noises; these too are modulated by the local oscillator power fluctuations. Note that when $\varepsilon = 1/2$ the local oscillator quantum noise contribution vanishes.

Let us further specialize the quantum results by supposing that the only excited mode of $\hat{F}_S$ is the monochromatic plane-wave pulse $(A_dT)^{-1/2}$ for $\overline{x\varepsilon}A_d$, $t\varepsilon T$, and that $\hat{a}_S$ is the annihilation operator for this mode. Matched filtering of the differenced output currents then yields a measurement of

$$\hat{M} \equiv e^{-1}\int_0^T [\hat{i}_1(t) - \hat{i}_2(t)]dt \ , \tag{85}$$

where normalization by the electron charge has been used, for convenience, to make the observation values dimensionless. We assume that the mean function and covariance function of the stationary complex-Gaussian local-oscillator random process

$$\underline{Y}(t) \equiv (P_{LO}(t)/h\nu_o A_d)^{1/2} \exp(-j\phi_{LO}(t)) \tag{86}$$

are

$$\eta_{\underline{Y}} = [(1-\eta)\langle N_{LO}\rangle/A_dT]^{1/2} \ , \tag{87}$$

and

$$K_{\underline{yy}}(\tau) = (\gamma\langle N_{LO}\rangle/A_dT)k(\tau) \quad , \tag{88}$$

respectively, where $\langle N_{LO}\rangle$ is the average number of local oscillator photons present over A_dxT , $\gamma^{1/2}$ is the fractional root-mean-square (rms) local oscillator amplitude fluctuation level, and $k(\tau)$ is a real-valued normalized covariance ($k(0) = 1$). It then follows that

$$\langle\hat{M}\rangle = \eta(1-2\varepsilon)\langle N_{LO}\rangle + 4\eta[\varepsilon(1-\varepsilon)(1-\gamma)\langle N_{LO}\rangle]^{1/2}\ \langle\hat{a}_{S1}\rangle \ , \tag{89}$$

and

$$\begin{aligned}\langle\Delta\hat{M}^2\rangle &= \eta(1-\eta)\langle N_{LO}\rangle + \eta^2(1-2\varepsilon)^2\langle N_{LO}\rangle + 16\eta^2\varepsilon(1-\varepsilon)(1-\gamma)\langle N_{LO}\rangle\langle\Delta\hat{a}_{S1}{}^2\rangle \\ &+ [\eta(1-2\varepsilon)\langle N_{LO}\rangle/T]^2\int_{-T}^{T}d\tau[\gamma^2k^2(\tau) + 2\gamma(1-\gamma)k(\tau)]\ (T-|\tau|) \\ &+ (2\eta/T)^2(1-2\varepsilon)\gamma[\varepsilon(1-\varepsilon)\langle N_{LO}\rangle^3(1-\gamma)]^{1/2}\,2\,\langle\hat{a}_{S1}\rangle\int_{-T}^{T}d\tau k(\tau)(T-|\tau|) \\ &+ (2\eta/T)^2\varepsilon(1-\varepsilon)\gamma\langle N_{LO}\rangle[T^2+2\langle\hat{a}_S{}^{+}\hat{a}_S\rangle\int_{-T}^{T}d\tau k(\tau)(T-|\tau|)] \quad ,\end{aligned} \tag{90}$$

give the mean and variance of the $\hat{M}$ measurement from which a signal-to-noise ratio

$$SNR_{\hat{M}} \equiv \langle\hat{M}\rangle^2/\langle\Delta\hat{M}^2\rangle \tag{91}$$

may be calculated. In Eq. (89), the first term is the average local oscillator bias current contribution, and the second term is the average signal field mixing term contribution, where $\hat{a}_{S1} = (\hat{a}_S+\hat{a}_S{}^{+})/2$ for $\hat{a}_S$ the annihilation operator of the sole excited $\hat{F}_S$ mode. In Eq. (90), the first term is due to the $\eta<1$ noises n_{vac1} and n_{vac2} , the second term is due to the local oscillator quantum noise n_{LOq} , the third term is the signal field quantum noise, the fourth term is due to the local-oscillator power fluctuations, and

the last terms are due to the random modulation of the mixing current by the local oscillator fluctuations.

The previous dual-detector homodyne studies of Yuen and Chan [25] and Schumaker [30] assume $\epsilon = 1/2$, $(1-\gamma)\langle N_{LO}\rangle \gg 1$, and a slowly fluctuating local oscillator (corresponding, in our case, to $k(\tau) \approx 1$ for $|\tau| \leq T$). In this limit both prior studies find (in our notation)

$$SNR_M^{\wedge} = \frac{\langle \hat{a}_{S1} \rangle^2}{\langle \Delta \hat{a}_{S1}^2 \rangle + (1-\eta)/4\eta} \quad , \tag{92}$$

whereas we obtain

$$SNR_M^{\wedge} = \frac{\langle \hat{a}_{S1} \rangle^2}{\langle \Delta \hat{a}_{S1}^2 \rangle + (1-\eta)/4\eta(1-\gamma) + \gamma(1+2\langle \hat{a}_S^{\dagger} \hat{a}_S \rangle)/4(1-\gamma)} \quad . \tag{93}$$

For small fractional rms local-oscillator amplitude fluctuations ($\gamma \ll 1$), (93) differs from (92) because of an additional noise term in the denominator that is approximately $\gamma(1 + 2\langle \hat{a}_S^{\dagger} \hat{a}_S \rangle)/4$. Physically, this term arises from the random local-oscillator modulation of the mixing current, an effect neglected by the earlier studies. In order for this term to be insignificant compared to the signal quantum noise of a coherent state ($\langle \Delta \hat{a}_{S1}^2 \rangle = 1/4$), we require that

$$\gamma \langle \hat{a}_S^{\dagger} \hat{a}_S \rangle \ll 1 \quad , \tag{94}$$

i.e., the fractional rms local oscillator amplitude fluctuation must be much smaller than the square root of the reciprocal of the average number of signal field photons.[11] This requirement becomes even more stringent if a squeezed state is being probed, for which $\langle \Delta \hat{a}_{S1}^2 \rangle < 1/4$ prevails.

In addition to exhibiting the potentially significant random modulation of the mixing term, our formulation, (84), shows another effect suppressed in [25] and [30]. This is the random amplitude modulation of the local oscillator and $\eta < 1$ quantum noises by the classical amplitude noise of the local oscillator. Although this modulation does not explicitly enter the signal-to-noise ratio , it does make the last three terms in (84) non-Gaussian random processes, an effect which will modify digital communication error probability calculations somewhat.

Heterodyne Detection The semiclassical description for the differenced output currents in heterodyne detection is

$$\begin{aligned} i_1(t) - i_2(t) &= e\eta(1-2\varepsilon)P_{LO}(t)/h\nu_o \\ &+4e\eta[\varepsilon(1-\varepsilon)P_{LO}(t)/h\nu_o A_d]^{1/2}\mathrm{Re}\left(\int_{A_d} d\bar{x}F_S(\bar{x},t)e^{-j(2\pi\nu_{IF}t-\phi_{LO}(t))}\right) \\ &+e[\eta(1-\varepsilon)P_{LO}(t)/h\nu_o]^{1/2}\, n_{shot1}(t) \\ &-e[\eta\varepsilon P_{LO}(t)/h\nu_o]^{1/2} n_{shot2}(t) \ , \end{aligned} \tag{95}$$

and the quantum description is

$$\begin{aligned} i_1(t) - i_2(t) &= e\eta(1-2\varepsilon)P_{LO}(t)/h\nu_o \\ &+4e\eta[\varepsilon(1-\varepsilon)P_{LO}(t)/h\nu_o A_d]^{1/2}\mathrm{Re}\left(\int_{A_d} d\bar{x}\hat{F}_S(\bar{x},t)e^{-j(2\pi\nu_{IF}t-\phi_{LO}(t))}\right) \\ &+e\eta(1-2\varepsilon)(P_{LO}(t)/h\nu_o)^{1/2} n_{LOq}(t) \\ &+e[\eta(1-\eta)(1-\varepsilon)P_{LO}(t)/h\nu_o]^{1/2} n_{vac1}(t) \end{aligned}$$

$$-e[n(1-n)\varepsilon P_{LO}(t)/h\nu_o]^{1/2} n_{vac2}(t)$$

$$+en[2\varepsilon(1-\varepsilon)P_{LO}(t)/h\nu_o]^{1/2} n_{Iq}(t) \quad . \qquad (96)$$

These results differ from the corresponding homodyne results, (83) and (84), in only two respects. First, the mixing terms (second terms on the right in (95) and (96)) beat the signal field to an intermediate frequency not baseband, and so they sense both quadratures of the signal field. Second, the quantum result (96) gains a noise contribution from the image band quantum noise through $n_{Iq}(t)$. The local oscillator excess noise (and its cancellation when $\varepsilon = 1/2$) and the random modulation of the signal and noise terms by the local oscillator fluctuations thus continue to be present in the heterodyne case, i.e., the interpretations given for the homodyne situation apply here as well. Once again, the relevant previous work on dual detector systems [25], [28], [29] does not include all the effects contained in our treatment; the random local oscillator modulation of the signal and noise terms is absent in the above analyses.

As an illustration of these omissions, let us compare our semiclassical answer (95) assuming a deterministic monochromatic plane-wave pulse signal $F_S(\bar{x},t) = \alpha_S(A_d T)^{-1/2}$ for $\bar{x}\varepsilon A_d, t\varepsilon T$, with the corresponding $\varepsilon=1/2$, equal quantum efficiency result of Abbas and Chan [29]. The latter claim, in our notation, that the differenced output currents consist of a mean current

$$\langle(i_1(t) - i_2(t))\rangle = 2en\eta^{-1}\langle N_{LO}\rangle^{1/2} Re(\alpha_S e^{-j2\pi\nu_{IF}t}) \quad , \qquad (97)$$

embedded in an additive zero-mean white Gaussian noise process with bilateral spectral density

$$S(f) = e^2\eta\langle N_{LO}\rangle/T \quad . \qquad (98)$$

We have, using (86) - (87) in (95), that the differenced output currents consist

of a mean current

$$\langle (i_1(t) - i_2(t)) \rangle = 2en T^{-1} [(1-\gamma)\langle N_{LO} \rangle]^{1/2} \mathrm{Re}(\alpha_S e^{-j2\pi\nu_{IF}t}) \quad , \tag{99}$$

plus a <u>conditionally</u> non-stationary zero-mean white Gaussian shot noise process that, <u>given</u> the local oscillator power waveform, has covariance function

$$K(t,s) = e^2 \eta (P_{LO}(t)/h\nu_o)\delta(t-s) \quad , \tag{100}$$

plus a <u>signal dependent</u> zero-mean stationary Gaussian noise process

$$i''(t) = 2en(A_d/T)^{1/2} \mathrm{Re}[\alpha_S (\underline{y}(t) - m_{\underline{y}})^* e^{-j2\pi\nu_{IF}t}] \quad , \tag{101}$$

with covariance function

$$K_{i''i''}(\tau) = 2(en/T)^2 \gamma \langle N_{LO} \rangle |\alpha_S|^2 k(\tau) \cos(2\pi\nu_{IF}\tau) \quad . \tag{102}$$

When Eq.(100) is averaged over the P_{LO} statistics it reduces to a stationary white noise spectrum (98) , however the random P_{LO} fluctuations make the noise non-Gaussian, albeit in a minor way if $\gamma << 1$. The noise current $i''(t)$ comes from the random modulation of the mixing term and may present a significant degradation. Consider a high quality ($\gamma << 1$), slowly fluctuating local oscillator ($k(\tau) \approx 1$ for $|\tau| \leq T$) and the matched filter processor generating

$$M = e^{-1} \int_0^T (i_1(t) - i_2(t)) 2^{1/2} \cos[2\pi\nu_{IF}t - \arg(\alpha_S)] \, , \tag{103}$$

then the Abbas and Chan model gives a signal-to-noise ratio

$$SNR_M = 2\eta |\alpha_S|^2 \quad , \tag{104}$$

whereas we have that

$$SNR_M = \frac{2n|\alpha_s|^2}{1 + n\gamma|\alpha_s|^2} . \qquad (105)$$

As in the quantum homodyne example given earlier, at high average detected signal levels there is a very stringent requirement on local oscillator amplitude fluctuations if SNR degradation is to be avoided.

IV. DISCUSSION

At this point, we have clearly established how the quantum theory for coherent optical detection subsumes the familiar semiclassical statistics in a natural way. We have also seen that the quantum approach is essential for studying the photodetection statistics of non-classical field states. There is now considerable interest in a particular class of non-classical states, called the two-photon coherent states [14] or the squeezed states [15]. These states are in essence minimum uncertainty product states for the quadrature components of the photon-units field operator $\hat{E}(\bar{x},t)$. In particular, for a single field mode with annihilation operator $\hat{a}$, the two-photon coherent state $|\beta;\mu,\nu>$ obeys the eigenket relation

$$(\mu\hat{a} + \nu\hat{a}^{\dagger})|\beta;\mu,\nu> = \beta|\beta;\mu,\nu> , \qquad (106)$$

where β,μ,ν are complex numbers and μ,ν satisfy $|\mu|^2 - |\nu|^2 = 1$. With $\hat{a}_1 = (\hat{a} + \hat{a}^{\dagger})/2$ and $\hat{a}_2 = (\hat{a} - \hat{a}^{\dagger})/2j$ denoting the quadrature components of $\hat{a}$, we then find that the state $|\beta;\mu,\nu>$ gives

$$<\Delta\hat{a}_1^2> = |\mu - \nu|^2/4, \qquad (107a)$$

and

$$<\Delta\hat{a}_2^2> = |\mu + \nu|^2/4. \qquad (107b)$$

When μ,ν are real valued, (107) implies that $|\beta;\mu,\nu>$ satisfies the Heisenberg relation

$$<\Delta\hat{a}_1^2><\Delta\hat{a}_2^2> \geq 1/16 \qquad (108)$$

with equality, as does the familiar coherent state $|\alpha>$. Unlike the coherent state, which gives $<\Delta\hat{a}_1^2> = <\Delta\hat{a}_2^2> = 1/4$, (107) shows that there is an asymmetric noise division between the quadratures (a noise squeezing) in the state $|\beta;\mu,\nu>$, with the low-noise quadrature being less noisy than a coherent state. This noise reduction can be used, in principle, to effect important performance improvements in optical communications [16] - [19] and precision measurements [20] - [23].

As yet, there have been no experimental observations of squeezed state light. Theoretical studies, which employ varying degrees of idealization, indicate that such states may be generated by degenerate four-wave mixing (DFWM) [39] - [42], as well as a number of other nonlinear optical processes [14], [15], [43] - [46]. We are presently working on a continuous-wave DFWM experiment using homodyne detection to generate and verify the quadrature noise squeezing. In this experiment, a single frequency-stabilized laser will be used to provide all the input beams to the four-wave mixer, as well as the local oscillators for dual-detector homodyne detection. The results of this paper permit the expected photocurrent statistics for this experiment to be derived, including the effects of the laser's residual amplitude and phase fluctuations. Specifically, an iterated expectation approach is used, as in Section III. The photocurrent statistics are first obtained assuming the laser output to be a particular coherent state. This entails a calculation of the four-wave mixer output state, along the lines of [40], followed by a calculation of the sort performed here in Section IIIA. To average over the input laser fluctuations,

we assign to the coherent state value for this laser a classical probability distribution. We can then proceed as in Section IIIB, except that the state of the signal field operator in the homodyne apparatus is now dependent on the coherent-state value of the local-oscillator field in that apparatus, because both fields are derived from the same laser.

ACKNOWLEDGEMENT

This research was supported by Office of Naval Research Contract N00014-81-K-0662.

References

[1] M.C. Teich, "Infrared heterodyne detection," Proc. IEEE, vol. 56, pp. 37-46, January 1968.

[2] R.M. Gagliardi and S. Karp, Optical Communications, New York: Wiley, 1976, chap. 6.

[3] R.M. Kingston, Detection of Optical and Infrared Radiation, Berlin: Springer Verlag, 1978, chap. 3.

[4] R.C. Harney, ed., "Physics and technology of coherent infrared radar," Proc. Soc. Photo-Opt. Instrum. Eng., vol. 300, 1981.

[5] R.C. Harney, ed., "Coherent infrared radar systems and applications," Proc. Soc. Photo-Opt. Instrum. Eng., vol. 415, 1983.

[6] Y. Yamamoto and T. Kimura, "Coherent optical fiber transmission systems," IEEE J. Quantum Electron., vol. QE-17, pp. 919-935, June 1981.

[7] T.G. Hodgkinson, D.W. Smith, and R. Wyatt, "1.5 μm optical heterodyne systems operating over 30 km of monomode fibre," Electron. Lett., vol. 18, pp. 929-930, October 1982.

[8] Y. Bouidene, A. Leclert, D. Le Guen, M. Monerie, A. Perichon, J.C. Simon, and F. Favre, "DPSK heterodyne-type fiber communication experiment," in Globecom '83 Conference Record, New York: IEEE, 1983, pp. 720-724.

[9] V.W.S. Chan, "Coherent optical space communications system architecture and technology issues," Proc. Soc. Photo-Opt. Instrum. Eng., vol. 295, pp. 10-17, 1981.

[10] F.G. Walther, S.D. Lowney, and J.E. Kaufman, "Frequency tracking for heterodyne optical communications using semiconductor lasers," paper FC-3 in Digest of the Conference on Lasers and Electro-Optics, New York: IEEE, 1983.

References (Cont'd)

[11] P.L. Kelley and W.H. Kleiner, "Theory of electromagnetic field measurement and photoelectron counting," Phys. Rev., vol. 136, pp. A316-A334, October 1964.

[12] H.J. Kimble, M. Dagenais, and L. Mandel, "Photon antibunching in resonance fluorescence," Phys. Rev. Lett., vol. 39, pp. 691-695, September 1977.

[13] R. Short and L. Mandel, "Observation of sub-Poissonian photon statistics," Phys. Rev. Lett., vol. 51, pp. 384-387, August 1983.

[14] H.P. Yuen, "Two-photon coherent states of the radiation field," Phys. Rev. A, vol. 13, pp. 2226-2243, June 1976.

[15] D.F. Walls, "Squeezed states of light," Nature, vol. 306, pp. 141-146, November 1983.

[16] H.P. Yuen and J.H. Shapiro, "Optical communication with two-photon coherent states — part I: quantum-state propagation and quantum-noise reduction," IEEE Trans. Inform. Theory, vol. IT-24, pp. 657-668, November 1978.

[17] J.H. Shapiro, H.P. Yuen, and J.A. Machado Mata, "Optical communication with two-photon coherent states — part II: photoemissive detection and structured receiver performance," IEEE Trans. Inform. Theory, vol. IT-25, pp. 179-192, March 1979.

[18] H.P. Yuen and J.H. Shapiro, "Optical communication with two-photon coherent states — part III: quantum measurements realizable with photoemissive detectors," IEEE Trans. Inform. Theory, vol. IT-26, pp. 78-92, January 1980.

[19] J.H. Shapiro, "Optical waveguide tap with infinitesimal insertion loss," Opt. Lett., vol. 5, pp. 351-353, August 1980.

[20] C.M. Caves, "Quantum mechanical noise in an interferometer," Phys. Rev. D, vol. 23, pp. 1693-1708, April 1981.

References (Cont'd)

[21] C.M. Caves, "Quantum limits on noise in linear amplifiers," Phys. Rev. D, vol. 26, pp. 1817-1839, October 1982.

[22] J.H. Shapiro and S.S. Wagner, "Phase and amplitude uncertainties in heterodyne detection," IEEE J. Quantum Electron., vol. QE-20, pp. xxx-xxx, July 1984.

[23] R.S. Bondurant and J.H. Shapiro, "Squeezed states in phase-sensing interferometers," submitted to Phys. Rev. D.

[24] R.J. Cook, "Photon dynamics," Phys. Rev. A, vol. 25, pp. 2164-2167, April 1982.

[25] H.P. Yuen and V.W.S. Chan, "Noise in homodyne and heterodyne detection," Opt. Lett., vol. 8, pp. 177-179, March 1983; errata, Opt. Lett., vol. 8, p. 345, June 1983.

[26] R.V. Pound, Microwave Mixers, New York: McGraw-Hill, 1948, chap. 6.

[27] R.E. Collin, Foundations for Microwave Engineering, New York: McGraw-Hill, 1966, pp. 285-286.

[28] G.L. Abbas, V.W.S. Chan, and T.K. Yee, "Local-oscillator excess-noise suppression for homodyne and heterodyne detection," Opt. Lett., vol. 8, pp. 419-421, August 1983.

[29] G.L. Abbas and V.W.S. Chan, "Optical design and performance of a dual-detector optical heterodyne receiver for local oscillator noise suppression," in Globecom '83 Conference Record, New York: IEEE, 1983, pp. 422-427.

[30] B.L. Schumaker, "Noise in homodyne detection," Opt. Lett., vol. 9, pp. 189-191, May 1984.

[31] R.M. Gagliardi and S. Karp, Optical Communications, New York: Wiley, 1976, chap. 2.

References (Cont'd)

[32] L. Mandel, "Fluctuations of photon beams and their correlations," Proc. Phys. Soc. (London), vol. 72, pp. 1037-1048, 1958.

[33] C.W. Helstrom, "Detectability of coherent optical signals in a heterodyne receiver," J. Opt. Soc. Am., vol. 57, pp. 353-361, March 1967.

[34] D.L. Snyder, Random Point Processes, New York: Wiley, 1975, pp. 178-185.

[35] W.B. Davenport and W.L. Root, Random Signals and Noise, New York: McGraw-Hill, 1958, p. 123.

[36] J.P. Gordon and W.H. Louisell, "Simultaneous measurements of noncommuting observables," in P.L. Kelley, B. Lax, and P.E. Tannenwald, eds., Physics of Quantum Electronics, New York: McGraw-Hill, 1966, pp. 833-840.

[37] H.P. Yuen, "Generalized quantum measurements and approximate simultaneous measurements of noncommuting observables," Phys. Lett., vol. 91A, pp. 101-104, August 1982.

[38] D.L. Snyder, Random Point Processes, New York: Wiley, 1975, pp. 23-24.

[39] H.P. Yuen and J.H. Shapiro, "Generation and detection of two-photon coherent states in degenerate four-wave mixing," Opt. Lett., vol. 4, pp. 334-336, October 1979.

[40] R.S. Bondurant, P. Kumar, J.H. Shapiro, and M. Maeda, "Degenerate four-wave mixing as a possible source of squeezed-state light," Phys. Rev. A, vol. 30, pp. xxx-xxx, July 1984.

[41] M.D. Reid, and D.F. Walls, "Quantum statistics of degenerate four-wave mixing," submitted for publication.

[42] P. Kumar and J.H. Shapiro, "Squeezed state generation via forward degenerate four-wave mixing," submitted to Phys. Rev. A.

[43] G. Milburn and D.F. Walls, "Production of squeezed states in a degenerate parametric amplifier," Opt. Commun., vol. 39, pp. 401-404, November 1981.

[44] L.A. Lugiato and G. Strini, "On the squeezing obtainable in parametric oscillators and bistable absorption," Opt. Commun., vol. 41, pp. 67-70, March 1982.

References (Cont'd)

[45] W. Becker, M.O. Scully, and M.S. Zubairy, "Generation of squeezed coherent states via a free-electron laser," Phys. Rev. Lett., vol. 48, pp. 475-477, February 1982.

[46] L.A. Lugiato and G. Strini, "On nonclassical effects in two-photon optical bistability and two-photon laser," Opt. Commun., vol. 41, pp. 374-378, May 1982.

Footnotes

1. The convention we use for this Fourier transform is necessitated by the accepted quantum-optics definition for what constitutes a positive-frequency field.
2. For a photomultiplier tube, the internal current gain amplifies the current we are analyzing by a sufficient amount to warrant its treatment as a classical entity. In the coherent optical detection cases that follow, the mixing gain produced by the strong local oscillator has a similar effect, see [22].
3. A classical state is either a Glauber coherent state or a classically random mixture of such states. In either case, the density operator ρ has a proper P-representation (17). The terminology arises, see below, because a classical state ρ gives rise to the same statistics in quantum photodetection theory as found for a classical field in semiclassical photodetection theory.
4. Because our idealized detector model neglects internal noise sources (dark current shot noise, thermal noise, etc.) N from Eq. (21) corresponds to the output of a pulse-discriminator/counter applied to the output current $\int_{A_d} d\bar{x}\, J(\bar{x},t)$. In other words, Eq. (21) models the output of an ideal (unity quantum efficiency) photomultiplier-tube/pulse-counter setup.
5. Our choice for the beam splitter transformation agrees with that employed in [18], and implies that the field leaving the other port of this optical element is $-(1-\varepsilon)^{1/2}E_S(\bar{x},t)+\varepsilon^{1/2}E_{LO}(\bar{x},t)$. Other beam splitter relations (see, e.g. [25] , [30]) are equivalent to ours after redefinition of the input and output planes.
6. A critical aspect of the strong local oscillator condition acting through the measurement operator (48) is that the mean local oscillator field and its

quantum noise both contribute to J_{hom} through the direct detection term, but only the mean local oscillator field (not its quantum noise) contributes to J_{hom} through the mixing term.

7. Very interesting noise reductions can accrue when the signal and image bands are quantum-mechanically dependent [22].

8. Because the in-phase and quadrature components of $\hat{F}_S$ are non-commuting observables, the image band noise enters into heterodyning in order to enforce the Heisenberg uncertainty principle on ideal simultaneous observations of these incompatible quantities (see [36], [37]).

9. Implicit in this conditioning statement is the fact that the local oscillator must, with very high probability, remain sufficiently strong to ensure the validity of the Section II theory. Also note that the signal field statistics may depend on the value of the local oscillator field, such as occurs in a laboratory experiment when the same laser is used to obtain both the signal and local oscillator beams (see Section IV).

10. The local oscillator fluctuations must not be such as to invalidate the Section II theory for any state $|\alpha_{LO}\rangle$ that occurs with appreciable probability. Also, the signal state (density operator) may depend on the value of the local oscillator field, if, for example, both beams originate from the same laser (see Section IV).

11. For example, to keep this added noise below 10% (in standard deviation) of the coherent-state signal quantum noise when $\langle \hat{a}_S^{\dagger} \hat{a}_S \rangle = 10^4$, we can tolerate no more than 0.3% local oscillator amplitude fluctuation. This limitation may be significant in precision measurement applications for which signal-to-noise ratios far in excess of 40dB are sought.

Figure Captions

Fig. 1 Geometry of an idealized surface photoemitter of active region A_d.

Fig. 2 Configuration for optical homodyne detection.

Fig. 3 Configuration for optical heterodyne detection.

Fig. 4 Configuration for dual-detector coherent optical detection.

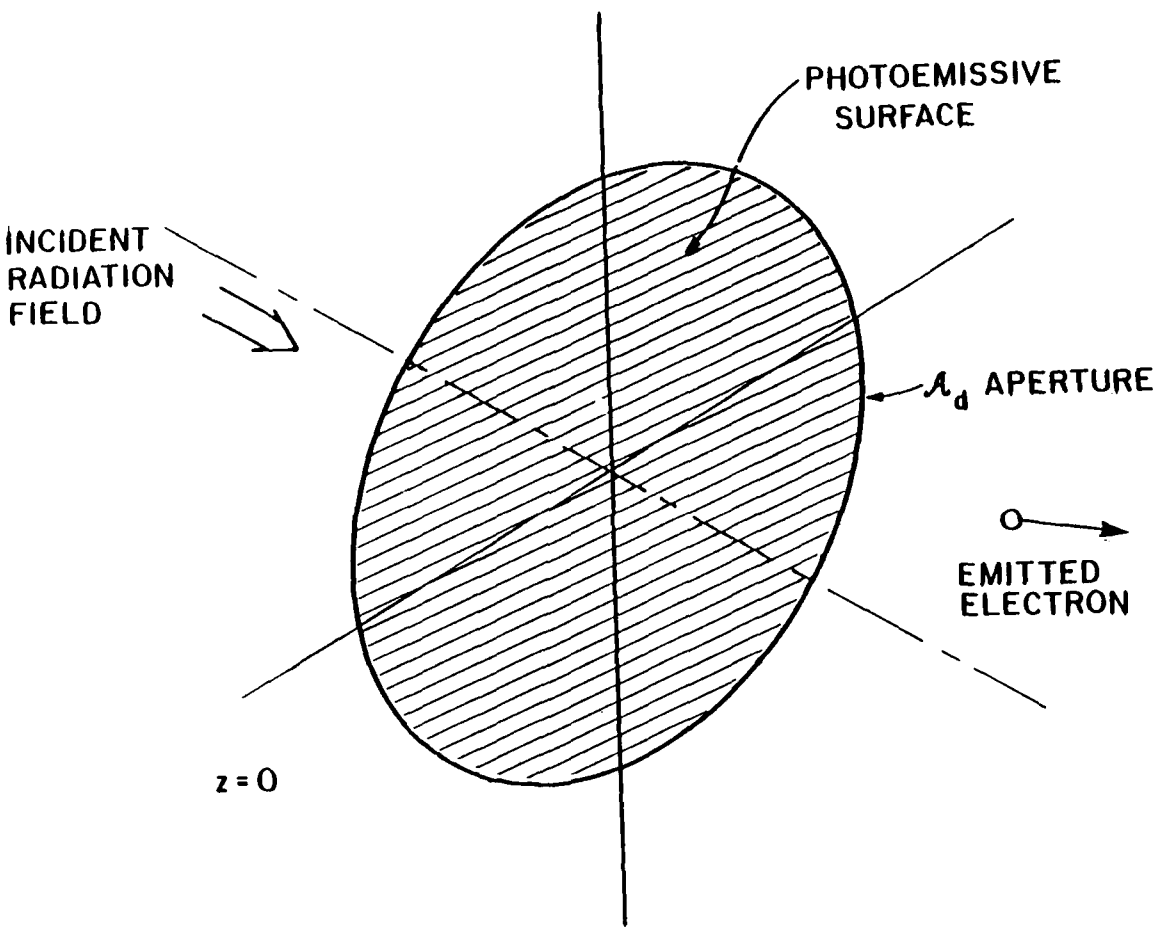

J.H. Shapiro Figure 1

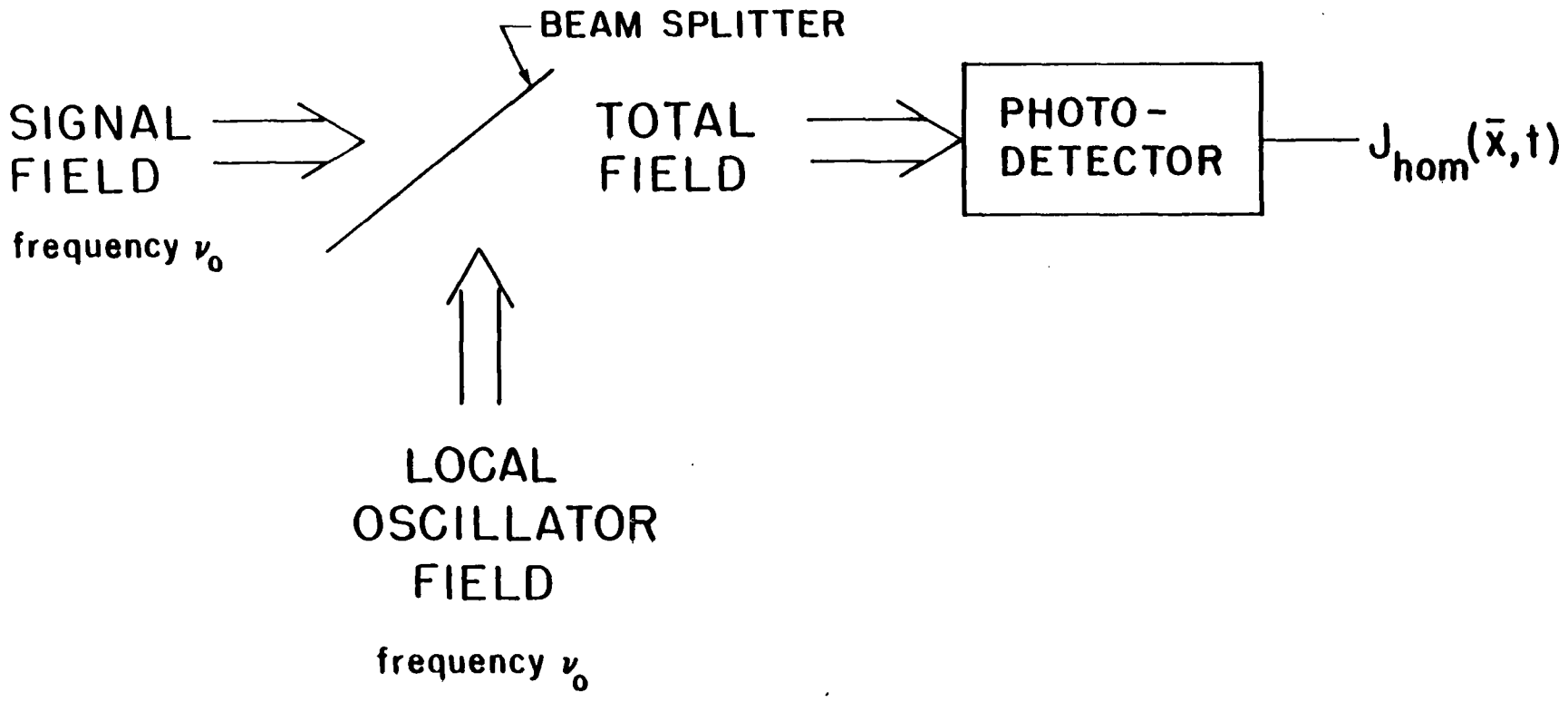

J. H. Shapiro Figure 2

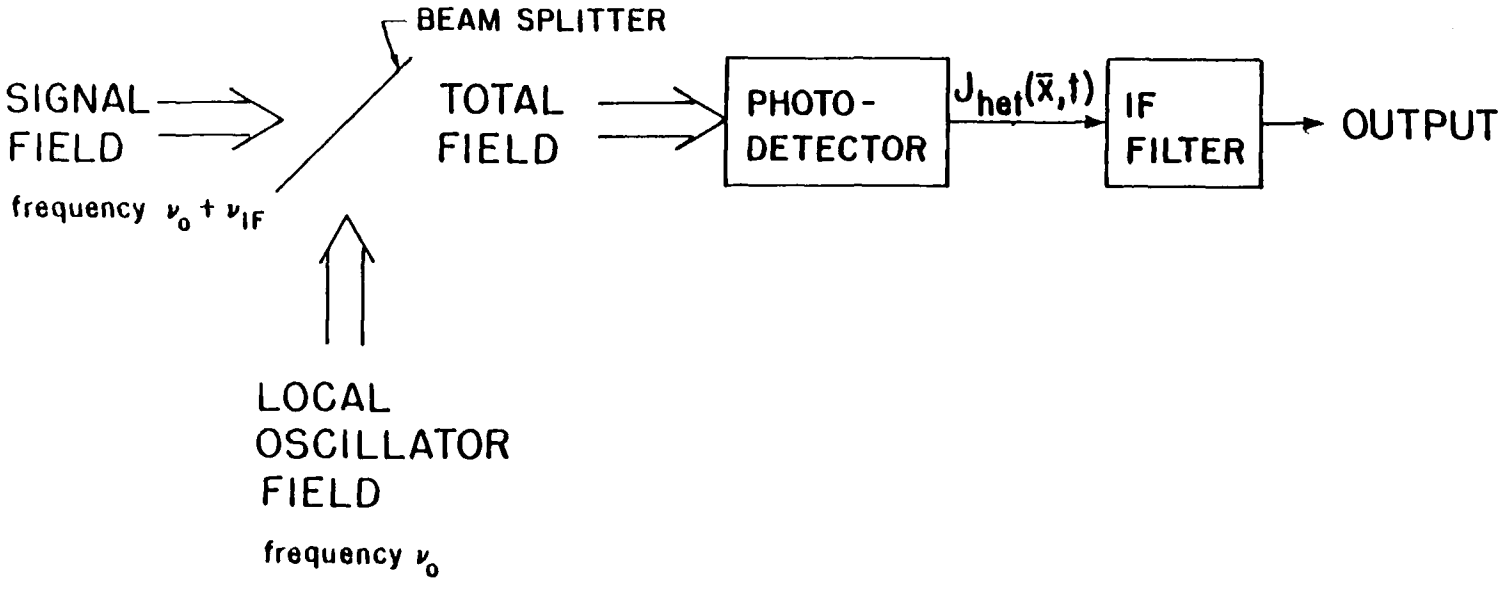

J.H. Shapiro Figure 3

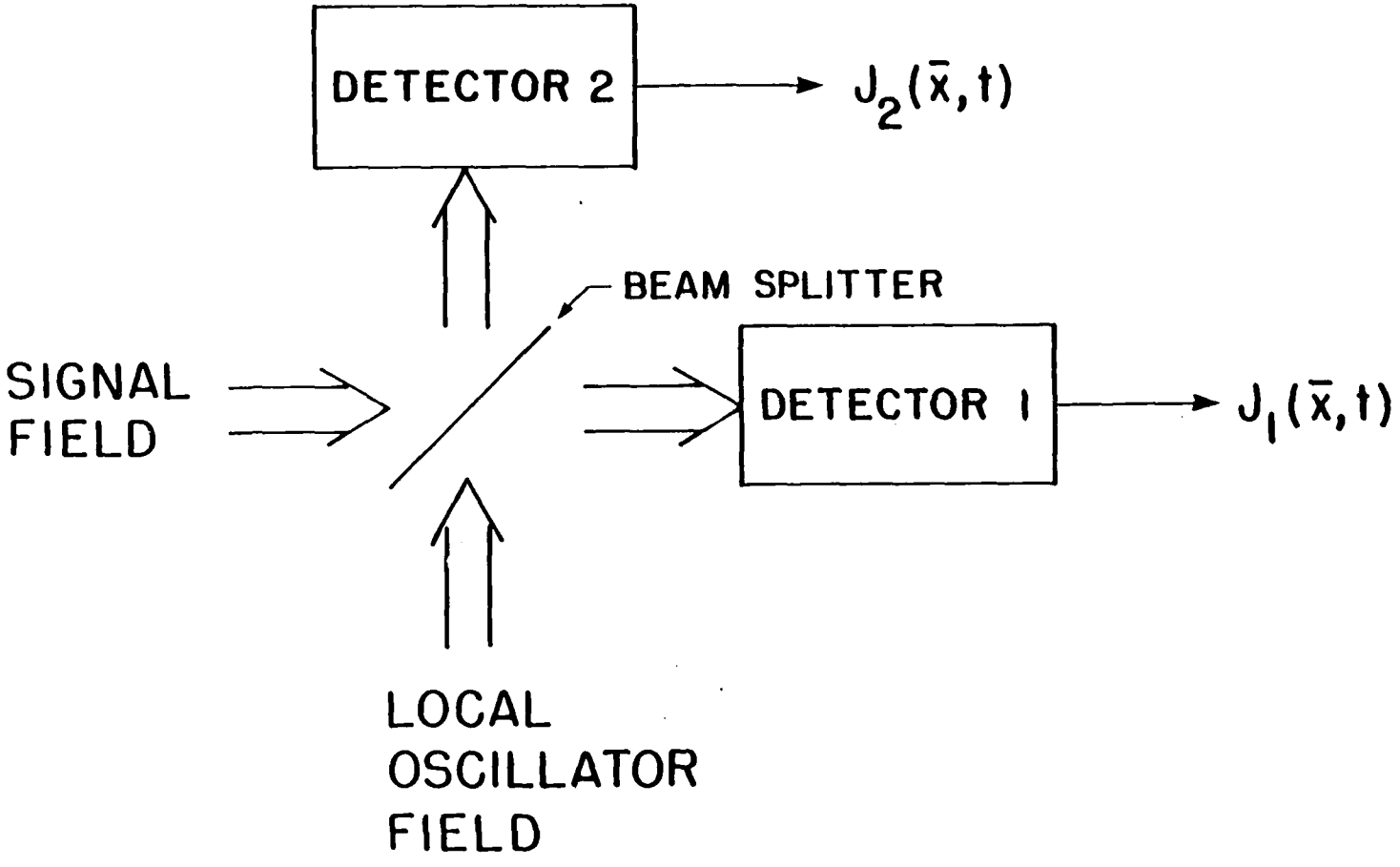

J.H. Shapiro Figure 4

APPENDIX III

DEGENERATE FOUR-WAVE MIXING LINESHAPES IN SODIUM VAPOR UNDER PULSED EXCITATION

Prem Kumar

Research Laboratory of Electronics
Massachusetts Institute of Technology
Cambridge, MA 02139

ABSTRACT

Degenerate four-wave mixing (DFWM) lineshapes are investigated in sodium vapor near the D_2 resonance line using nearly Fourier transform limited pulses. At low pump intensities sub-Doppler resolution is obtained. When the Rabi frequency associated with the pump intensity becomes equal to the ground state hyperfine frequency separation of sodium, each component of the double-peaked DFWM spectrum further splits into two components each. Adiabatic following model explains the near-resonant intensity dependence of the DFWM signal but is insufficient to explain the whole structure.

Resonant degenerate four-wave mixing (DFWM) has been shown to be an efficient technique for the generation of phase conjugate wave fronts[1]. In backward configurations, where the two pump beams as well as the two signal (probe and conjugate) beams counter-propagate to each other, the DFWM spectrum is Doppler free and has been used for high resolution spectroscopy[2]. However, true spectral information is obtained only when the pump beam intensities are small compared to the saturation intensity of the resonant medium. At higher pump intensities, complicated line shapes are observed; in particular, the line broadens and splits into two components. Several experimental and theoretical studies of this behavior have appeared in recent literature[3]. Most of the studies have employed cw lasers and hence steady state analyses have been used to explain the observed behavior.

The early experiments on resonant DFWM employed pulsed dye lasers[4]. DFWM spectrum in this case is also complicated and shows a dip to zero at the line center. Bloom et al. were the first to observe such a line shape. In the pulsed case, fluctuations (pulse to pulse energy, pulse-shape, and center frequency fluctuations) and other nonlinear effects such as self focussing complicate the line shape even further. Recently we have measured the DFWM line shapes with a pulsed dye laser system which was stabilized in center frequency and bandwidth. Our control of the fluctuations in the DFWM signal was essential for the measurement of the photon counting statistics of light generated via DFWM[5]. In this letter we describe the results of a study of DFWM line shapes with such a source.

The experimental setup is essentially the same as that in Ref. 6 and is shown in Fig. 1. An externally stabilized cw ring dye laser (sub MHz line width) is amplified through a chain of pulsed dye laser amplifiers pumped by the smoothed output of a Nd:YAG laser[7]. The output pulses of 4 ns duration with typically 10-20% energy fluctuations and a total line width of 200 MHz which is approximately twice the Fourier transform limited line width are used to perform DFWM.

About 10-50 MW/cm^2 pulse intensities are available from such a system. Backward DFWM geometry is employed with orthogonally polarized pump beams[8]. Phase conjugate (PC) signal whose polarization is orthogonal to the probe beam (PB) is separated using a polarization beam splitter (PBS) and directed onto a photomultiplier (PMT) whose output is sent to a boxcar integrator. The output of the boxcar which is proportional to the PC pulse energy goes to the y-axis of a chart recorder whose x-axis is swept with the dye laser frequency. The boxcar whose gate duration is chosen to be 80 ns is triggered optically. The PC signal is first delayed optically and then electrically using a 50 Ω cable inserted between the PMT and the boxcar in such a way that it arrives in the middle of the gate duration.

DFWM is performed in sodium vapor generated in a heat-pipe oven. It is maintained at 310°C implying a sodium vapor density of 4×10^{14} atoms/cm^3 for the measurements reported in this letter. 2.2 Torr of helium is used as the buffer gas. All the beams arrive in time coincidence at the sodium cell. The dye laser frequency is scanned over 10 GHz across the sodium D_2 line. The spectra obtained in this way are shown in Fig. 2 as a function of the pump beams intensities which are kept the same (to within 10%) for both the pumps. Appropriate neutral density filters are introduced in the probe beam path to avoid saturation of the PMT. The probe pulse energy is kept less than a few percent of the pump pulse energy in all cases to avoid pump depletion.

At the lowest pump intensities used of 0.3 kW/cm^2 (all relative intensity measurements are ± 10%)[9], the line shape consists of two peaks which are 4.5 GHz apart as shown in Fig. 2a. Also shown is the fluorescence observed in a direction making a small angle (≈1°) with the PC beam. The pulse widths (FWHM) are 0.74 and 0.83 GHz for the lower and the higher frequency peaks respectively. Therefore sub-Doppler resolution is obtained at these pump intensities even though the peaks occur away from the center of the Doppler-broadened line of width 1.8 GHz.

As the pump intensities are increased to 0.6 kW/cm^2, the higher frequency peak splits into two components separated by 1.3 GHz as shown in Fig. 2b. A further increase of the pump intensities to 1.9 kW/cm^2 leads to a splitting in the lower frequency peak as well, as shown in Figs. 2c and 2d. In Fig. 2d the reflectivity at the highest frequency peak is 0.7%. The reason for such a low reflectivity is because a relatively large angle was chosen between the pumps and the probe beam[2]. This choice was dictated by the low background requirement in our DFWM quantum noise measurements reported earlier[5]. With smaller angle and higher pump intensities (at least an order of magnitude higher than those reported herein) we have observed reflectivities as large as 700. Under these conditions the conjugate pulse duration is significantly shorter than the probe pulse duration. A systematic study of this behavior has recently been reported[10].

At still higher pump intensities of 3-10 kW/cm^2, only two peaks remain as shown in Figs. 2e and 2f. A further increase of the pump intensities leads to a broadening and weakening of the lower frequency peak which is consistent with the observations of earlier workers. A slight broadening and weakening is already observable in Fig. 7g. Jabr et al.[4] did not observe the lower frequency peak with the same choice of the pump and probe beam polarizations that we employ. Their pump intensities were at least an order of magnitude larger than ours. At high pump intensities, self-defocussing of the pump beams on the lower frequency side of the resonance causes a reduction of the actual pump intensities in the mixing medium, which results in a lowering of the PC signal.

The splitting of the DFWM lineshape (Figs. 2b-2d) was not observed in earlier experiments[4]. This we believe is because we have used stable center frequency nearly Fourier transform limited pulses for the above measurements[6]. Furthermore, at low intensities sub-Doppler lines whose widths are limited by power broadening are observed.

The nonlinearity responsible for DFWM in sodium vapor is due to resonantly enhanced electronic Kerr effect. Grischkowsky et al.[4] used the adiabatic following (AF) model for a two level atom under pulsed excitation to derive an expression for the DFWM reflectivity as a function of the pump intensities and detuning. When the AF conditions are satisfied,[11] the third order nonlinear susceptibility is given by

$$\chi^{(3)} = - \frac{N\mu^4 A^2}{h^3(\nu-\nu_0)^3 (1+A^2/A_s^2)^{3/2}} \qquad (1)$$

where μ is the electric dipole moment of the two level atom, A is the pump fields amplitudes (assumed equal for both the pumps), $\nu-\nu_0$ is the detuning of the DFWM frequency from the atomic line center frequency, N is the total number of atoms per unit volume, and A_s^2 is the normalized saturation intensity given by $A_s = h|(\nu-\nu_0)|/\mu$. The DFWM reflectivity is given by $R = \tan^2 \kappa L \simeq \kappa^2 L^2$ where $\kappa = 2\pi\nu\chi^{(3)}/2cn$, n is the linear refractive index of the medium, L is the interaction length, and the approximation is valid under conditions of weak reflectivity.

As the pump intensities are increased, the DFWM signal saturates because of the saturation of $\chi^{(3)}$. This is verified for a detuning of 2.3 GHz where the AF conditions are satisfied as shown in Fig. 3. DFWM reflectivities were measured from Fig. 2 at a detuning marked by the arrows. Dots are the experimental data and the solid line is a fit to Eq. (1) for $I_s = 7.8$ kW/cm^2 which agrees well with $I_s = \varepsilon_0 c(h(\nu-\nu_0)/\mu)^2/2 = 2.1$ kW/cm^2. Thus a good agreement is obtained with the AF model in its region of validity.

The detailed lineshapes cannot be predicted using the AF model as it is not valid sufficiently close to resonance. Steady state models[3] developed to explain cw DFWM lineshapes cannot be applied in the transient case of our experiment.

The splitting of the DFWM lineshape as shown in Figs. 2b-2d occurs when the Rabi frequency corresponding to the pump intensities is close to the ground state hyperfine splitting of the sodium atom which is 1.77 GHz. Moreover, the splitting of the lower frequency peak occurs at approximately twice the pump intensities than that of the higher frequency peak. This suggests that the multiple level nature of the sodium atom is playing a role. This is not surprising because the spectrum of the pulses used in this experiment is much narrower than the ground state hyperfine splitting of sodium. For our 200 MHz, 4 ns pulses, sodium can be well modelled as a three level atom of Λ type. The DFWM mechanism in our experiment is more complicated than it seems because at low pump intensities of Fig. 2a, although sub-Doppler resolution is obtained, the peaks are not separated by 1.77 GHz as would be the case in a cw DFWM experiment when the spectrum of the laser used is much narrower than the ground state hyperfine splitting. A detailed comparison with the theory can only be made when Maxwell-Bloch equations are solved in the transient regime for the backward DFWM configuration taking the three level nature of the medium into account.

This research was supported in part by the Office of Naval Research.

References:

1. R.L. Abrams and R.C. Lind, Opt. Lett. 2, 94 (1978); 3, 205 (1979); P.F. Liao, D.M. Bloom, and N.P. Economou, Appl. Phys. Lett. 32, 813 (1978); R.C. Lind and D.G. Steel, Opt. Lett. 6, 554 (1981); R.A. McFarlane and D.G. Steel, Opt. Lett. 8, 208 (1983).

2. L.M. Humphrey, J.P. Gorden, and P.F. Liao, Opt. Lett. 5, 56 (1980); D.G. Steel and J.F. Lam, Opt. Commun. 40, 77 (1981).

3. J.P. Woerdman and M.F.H. Schuurmans, Opt. Lett. 6, 240 (1981); P. Aubourg, J.P. Bettini, G.P. Agarwal, P. Cottin, D. Guerin, O. Meunier, and J.L. Boulnois, Opt. Lett. 6, 383 (1981); G.P. Agarwal, A. Van Lerberghe, P. Aubourg, and J.L. Boulnois, Opt. Lett. 7, 540 (1982); J.L. Boulnois, P. Aubourg, A. Van Lerberghe, and G.P. Agarwal, Appl. Phys. Lett. 42, 225 (1983); D. Bloch, R.K. Raj, K.S. Peng, and M. Ducloy, Phys. Rev. Lett. 49, 719 (1982); D. Bloch and M. Ducloy, J. Opt. Soc. Am. 73, 635 (1983); M. Ducloy and D. Bloch, Opt. Commun. 47, 351 (1983).

4. D.M. Bloom, P.F. Liao, and N.P. Economou, Opt. Lett. 2, 58 (1978); D. Grischkowsky, N.S. Shiren, and R.J. Bennett, Appl. Phys. Lett. 33, 805 (1978); D.G. Steel, R.C. Lind, J.F. Lam, and C.R. Giuliano, Appl. Phys. Lett. 5, 377 (1979); S.N. Jabr, L.K. Lam, and R.W. Hellwarth, Phys. Rev. A 24, 3264 (1981).

5. P. Kumar, R.S. Bondurant, J.H. Shapiro, and M.M. Salour in Coherence and Quantum Optics V, L. Mandel and E. Wolf (eds.), Plenum, New York, 1983, pp. 43-50; R.S. Bondurant, P. Kumar, J.H. Shapiro, and Mari Maeda, Phys. Rev. A, in Press.

6. P. Kumar, J.H. Shapiro, and R.S. Bondurant, Opt. Commun. 50, 183 (1984).

7. P. Kumar and R.S. Bondurant, Appl. Opt. 22, 1284 (1983).

8. D.G. Steel, R.C. Lind, J.F. Lam, and C.R. Giuliano, Appl. Phys. Lett. 35, 376 (1979).

9. All intensity measurements refer to peak intensities of the pulses which are spatially in TEM_{00} mode. The absolute value could be off by as much as a factor of 5.

10. G. Grynberg, B. Kleinmann, M. Pinard, and F. Trehin, Opt. Commun. 47, 355 (1983).

11. D. Grischkowsky, in Physics of Quantum Electronics, Vol. II, eds. S.F. Jacobs, M. Sargent III, J.F. Scott and M.O. Scully (Addison-Wesley, Reading, 1975) p. 437-452. For nearly Fourier transform limited pulses, the AF condition is

$$\left|A^{-1}dA/dt + T_2^{-1}\left[1 + \{\mu A/h(\nu-\nu_o)\}^2\right]\right| << |\nu-\nu_o| \left[1 + \{\mu A/h(\nu-\nu_o)\}^2\right],$$

which is satisfied for 4 ns pulses with T_2^{-1} = 10 MHz and $|\nu-\nu_o|$ = 2.3 GHz.

Figure Captions:

1. Schematic of the experimental apparatus. YAG = frequency doubled Nd:YAG laser, DL = cw dye laser, M = total reflector, BS = beam splitter, DET = detector, HWP = half wave plate, PBS = polarization beam splitter, PMT = photo-multiplier tube, PC = phase conjugate beam, BP = backward pump beam, FP = forward pump beam, PB = probe beam.

2. DFWM lineshapes at various pump intensities. Vertical scale is arbitrary and is linearly proportional to the DFWM signal, plotter scale factors are labelled. Also superimposed are the fluorescence spectra in parts a, b, and g. Pump intensities are labelled in kW/cm^2 in each plot. Start frequency in parts f and g is slightly shifted.

3. Dependence of the DFWM signal on the pump intensities.

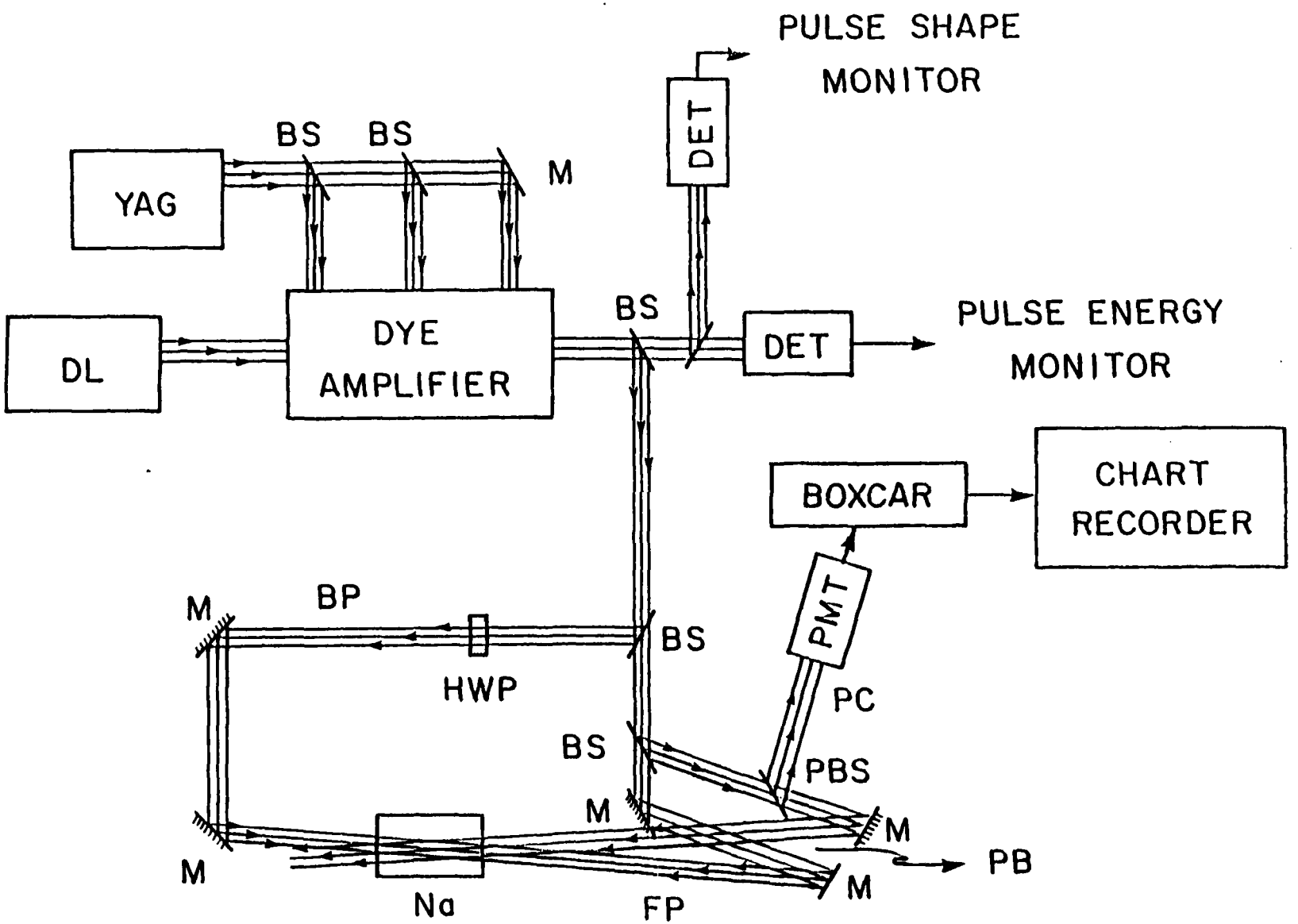
PULSE SHAPE
MONITOR
DET
BS
BS
M
YAG
DL
DYE
AMPLIFIER
BS
DET
PULSE ENERGY
MONITOR
BOXCAR
CHART
RECORDER
PMT
M
BP
BS
HWP
PC
BS
PBS
M
M
M
PB
M
Na
FP

Fig. 1

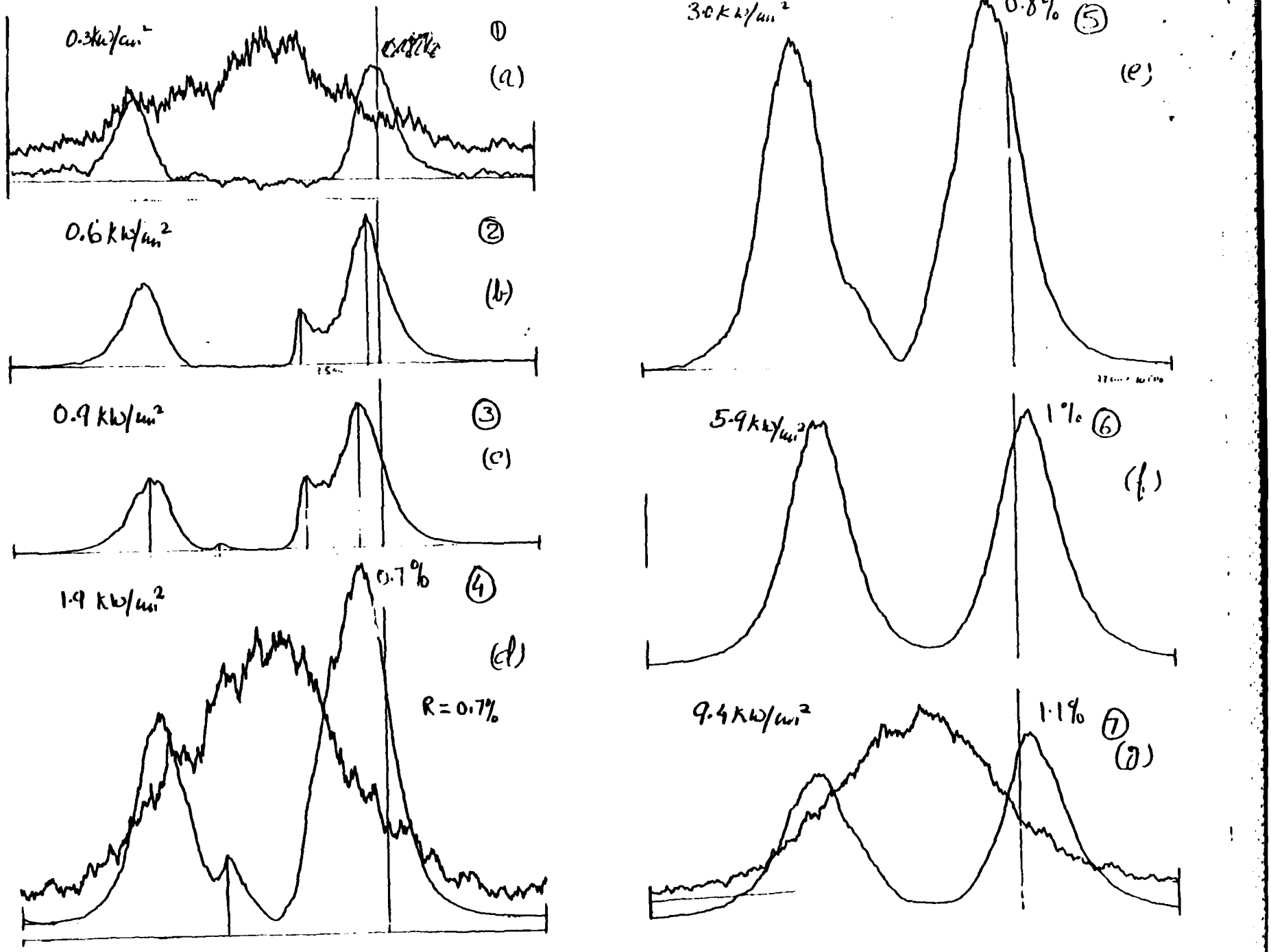
0.3 kw/cm²
①
(a)
0.6 kw/cm²
②
(b)
0.9 kw/cm²
③
(c)
1.9 kw/cm²
0.7%
④
(d)
R = 0.7%
3.0 kw/cm²
0.8%
⑤
(e)
5.9 kw/cm²
1%
⑥
(f)
9.4 kw/cm²
1.1%
⑦
(g)

Fig. 2

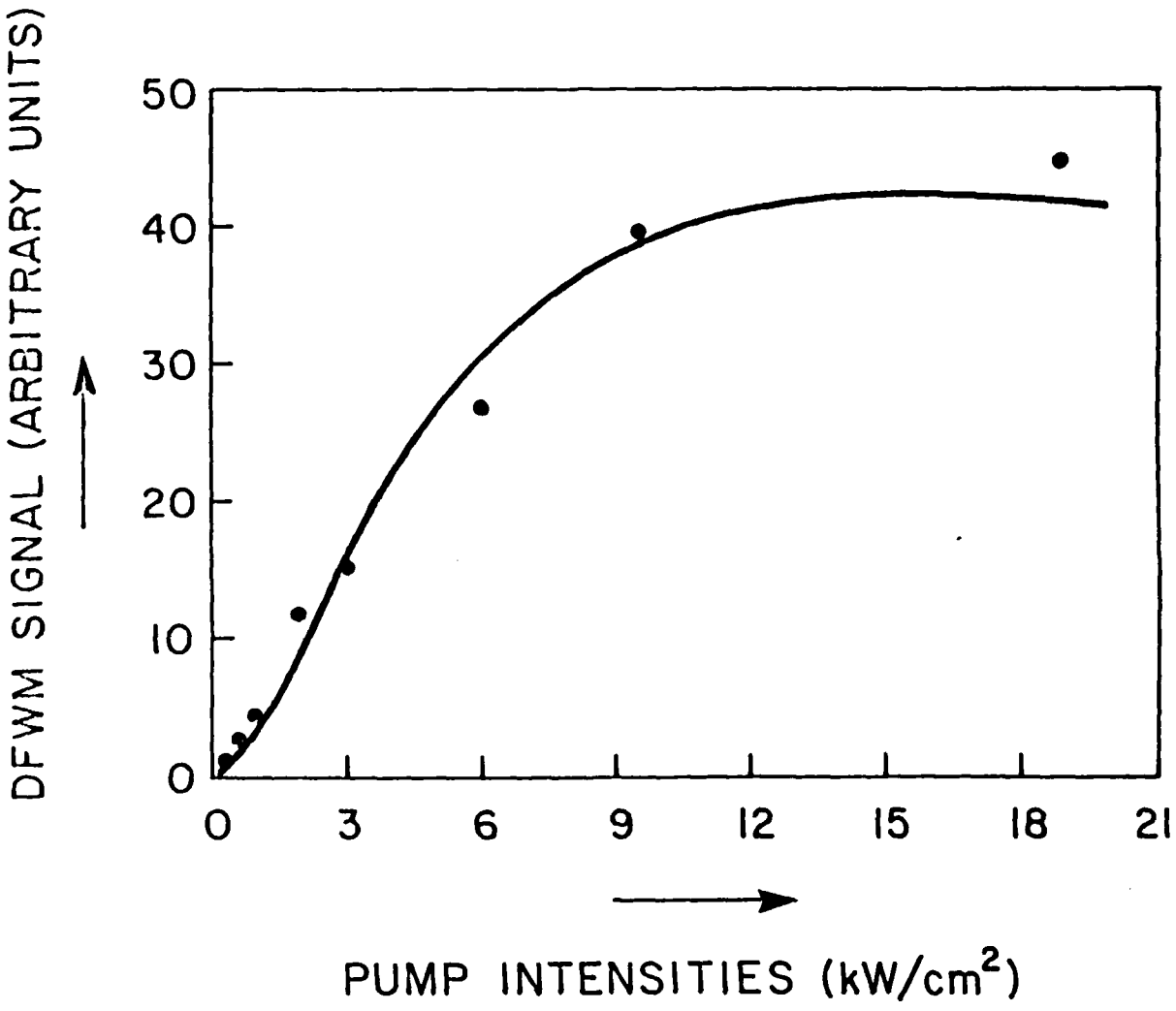
DFWM SIGNAL (ARBITRARY UNITS)
50
40
30
20
10
0
0
3
6
9
12
15
18
21
PUMP INTENSITIES (kW/cm^2)

Fig. 3

DISTRIBUTION LIST

	DODAAD Code	
Director Advanced Research Project Agency 1400 Wilson Boulevard Arlington, Virginia 22209 Attn: Program Management	HX1241	(2)
Director Earth and Environmental Physics Program Artic and Earth Sciences Division Office of Naval Research 800 North Quincy Street Arlington, Virginia 22217	N00014	(3)
Administrative Contracting Officer E19-628 Massachusetts Institute of Technology Cambridge, Massachusetts 02139	N66017	(1)
Director Naval Research Laboratory Attn: Code 2627 Washington, D.C. 20375	N00173	(6)
Defense Technical Information Center Bldg. 5, Cameron Station Alexandria, Virginia 22314	S47031	(12)
Office of Naval Research Eastern/Central Regional Office Bldg. 114, Sec. D 666 Summer Street Boston, Massachusetts 02210	N62879	(1)
TACTEC Battelle Memorial Institute 505 King Avenue Columbus, Ohio 43201	79986	(1)